ISSN 1617-2876

TOSHIBA MEDICAL SYSTEMS JOURNAL

TOSHIBA

Leading Innovation

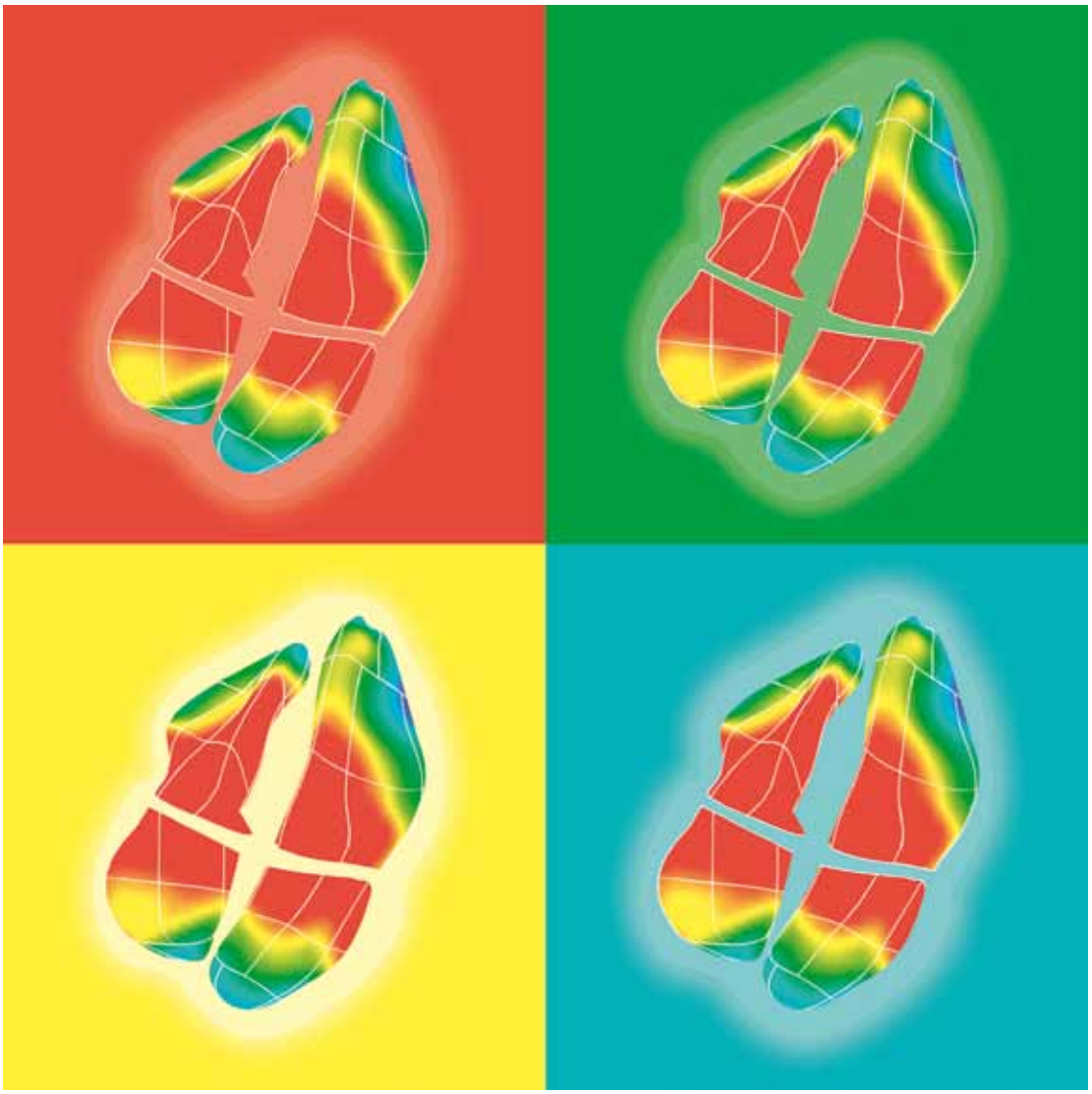

Ultrasound
2D and 3D Wall Motion Tracking in daily clinical practice

X-Ray
Investing today in radiology of tomorrow

MR
MR Imaging in MBD

CT
Adaptive Iterative Dose Reduction makes CT safer

VISIONS

16 · 2010

TOSHIBA MEDICAL SYSTEMS

An artist's adaptation of 3D Wall Motion Tracking data of all four heart chambers derived from a healthy volunteer using the Artida real-time 3D diagnostic ultrasound system.

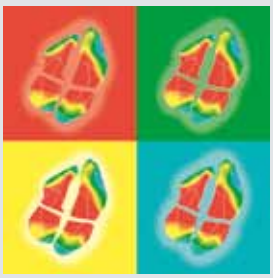

Imprint

Publisher:
TOSHIBA Medical Systems Europe B.V.,
Zilverstraat 1
NL-2718 RP Zoetermeer
Tel.: +31 79 368 92 22
Fax: +31 79 368 94 44
Email: visions@tmse.nl

Web site at:
www.toshiba-medical.eu

Editor-in-chief:
Jack Hoogendoorn
Modality coordinators:
CT: Roy Irwan
UL: Joerg Schlegel

Printing:
Frotscher Druck,
Darmstadt

FSC 100% From well-managed forests Cert no. SCS-COC-002224 www.fsc.org ©1996 Forest Stewardship Council

Subscription Service:
Email: visions@tmse.nl

Dear reader,

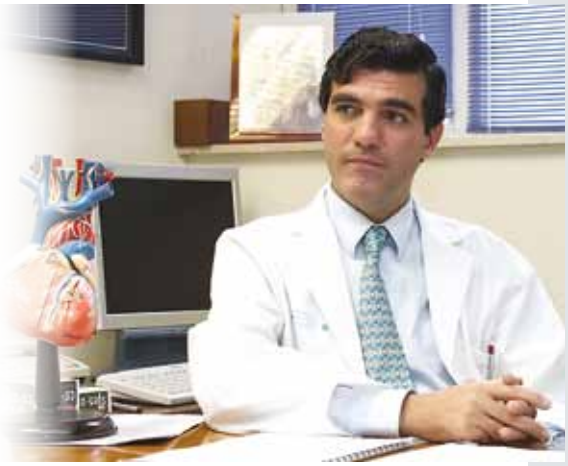

The assessment of left ventricular function is one of the most important aims in cardiovascular imaging. Current ultrasound guidelines recommend assessing global LV function by M-mode or 2D mode. Hence the development of 2D wall motion tracking (2D WMT) as a technique that records tissue motion based on natural acoustic markers in the ultrasonic image (speckles). This method has certainly improved the accuracy of the LV function analysis but still does not allow full assessment of the rather complex LV movement.

The introduction of 3D echocardiography into daily clinical practice has enabled the development of 3D wall motion tracking (3D WMT). This new method takes the full complexity of myocardial wall motion and anatomic structures into account, combining the benefits of wall motion tracking with outstanding ease of use and full quantitative assessment of myocardial wall motion.

Our own experience with this new technology shows that 3D WMT helps to reduce examination time, is very easy to use and allows a clearly superior evaluation of LV mechanics compared to other techniques. Similar to 2D WMT, 3D WMT can assess LV longitudinal and radial strain but is significantly faster, more comprehensive and more accurate. This issue of Visions contains three papers, including one from our institution, describing the accuracy and clinical usefulness of 3D WMT in daily clinical praxis.

But there are also articles on innovations in other modalities that, like 3D WMT, redefine the world of cardiac imaging. In CT, for example, on how to improve image quality by using a new reconstruction technique called AIDR. Or, in x-ray, how a new 30x30 cm detector enables maximum system utilisation in Australia.

Back to ultrasound: as illustrated on the cover of this magazine, 3D wall motion tracking is now even available for all cavities of the heart! This exciting development gives us plenty of opportunity to advance cardiovascular function assessment by studying and better understanding RV and atrial function.

You want to see 3D wall motion tracking, or any other cardiac innovation, in action? Then please go and visit the Toshiba booth at ESC 2010 (Zone C, C30:31).

Kind regards,

Prof. José Zamorano
Unidad de Imagen Cardiovascular
Hospital Clinico San Carlos
Madrid, Spain

The first Toshiba Ultimax-i 43x43 cm Flat Panel Detector was installed in Europe. Page 6

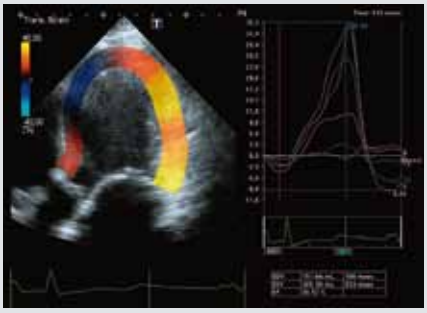

Speckle tracking is a new technique that allows the reliable analysis of myocardial movement and deformation. Unlike tissue Doppler, speckle tracking is independent of cardiac translation and insonation angle, as it is based on B-mode images. Page 18

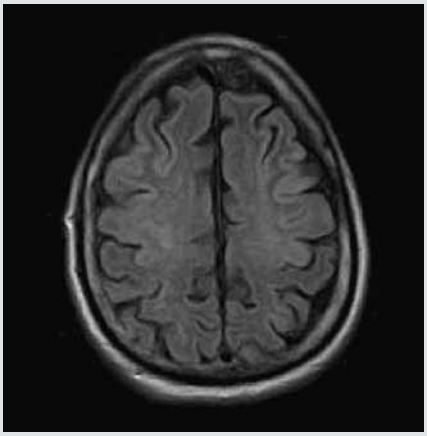

MR imaging of patients with acute Marchiafava-Bignami disease shows all the nectrotic changes in the brain. Page 22

3 Editorial

Interview

6 Interview with Dr JW Kuiper
Investing Today in the Radiology Department of Tomorrow

Ultrasound

10 AS Cerezo, L Pérez de Isla, J Rementería, W Gorissen, J Zamorano
3D Wall Motion Tracking: implementing a new tool in daily clinical practice

15 JC Hill, N Mehta, GP Aurigemma
Advanced Multi-Layer Speckle Strain Permits Transmural Myocardial Function Analysis in Health and Disease

18 T Wengenmayer
3D Speckle Tracking

20 M Rijken
Antenatal Ultrasound on a Bamboo Floor

MRI

22 A Schiavello, D Grisafi, C Reina
MR Imaging in Acute Marchiafava-Bignami Disease

News

24 Meanwhile at Toshiba

Computed Tomography

Introducing Aquilion ONE into an Emergency Department
Re-engineering the Patient Pathway 30

T Kühl, K Fuglsang Kofoed
Coronary Angiography and Myocardial Perfusion Imaging with 320-Detector Row CT Technology 32

IV Bodrova, EV Fominykh, NB Gagarina, EZ Mukhamatullina
First Experience with the 320-Row Detector in Otology 34

RMS Joemai
Improved Image Quality in Clinical CT by AIDR 38

X-Ray

Healthscope Allamanda Private Hospital
New 30x30 cm Detector with Compact Housing Enables Maximum System Utilisation 41

M Hanssen, O Poitier, P Couppié, F De Poli, P Leddet, P Angot
From Standard Coronary Angiography to Double Rotational Angiography 45

Toshiba Medical Systems
The New CV-3D plus Stent Planner, Stent Optimizer and Stent Fusion 51

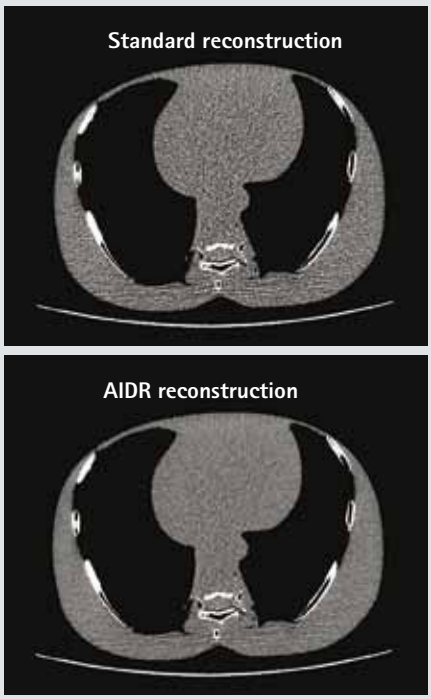

Reconstructions with AIDR, Adaptive Iterative Dose Reduction, compared to standard reconstructions show lower noise levels without loss of structures. Page 38

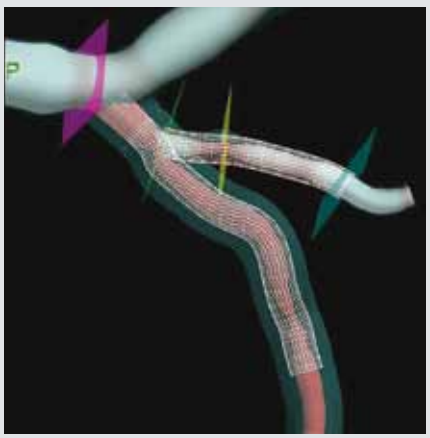

Toshiba's new CV-3D software package offers a unique function, Stent Planner, which shows a virtual stent over the 3D coronary arteries of the 3D QCA image. Page 51

Investing Today in the Radiology Department of Tomorrow

Customer feedback on working with the first Toshiba Ultimax-i 43x43 cm Flat Panel Detector installed in Europe

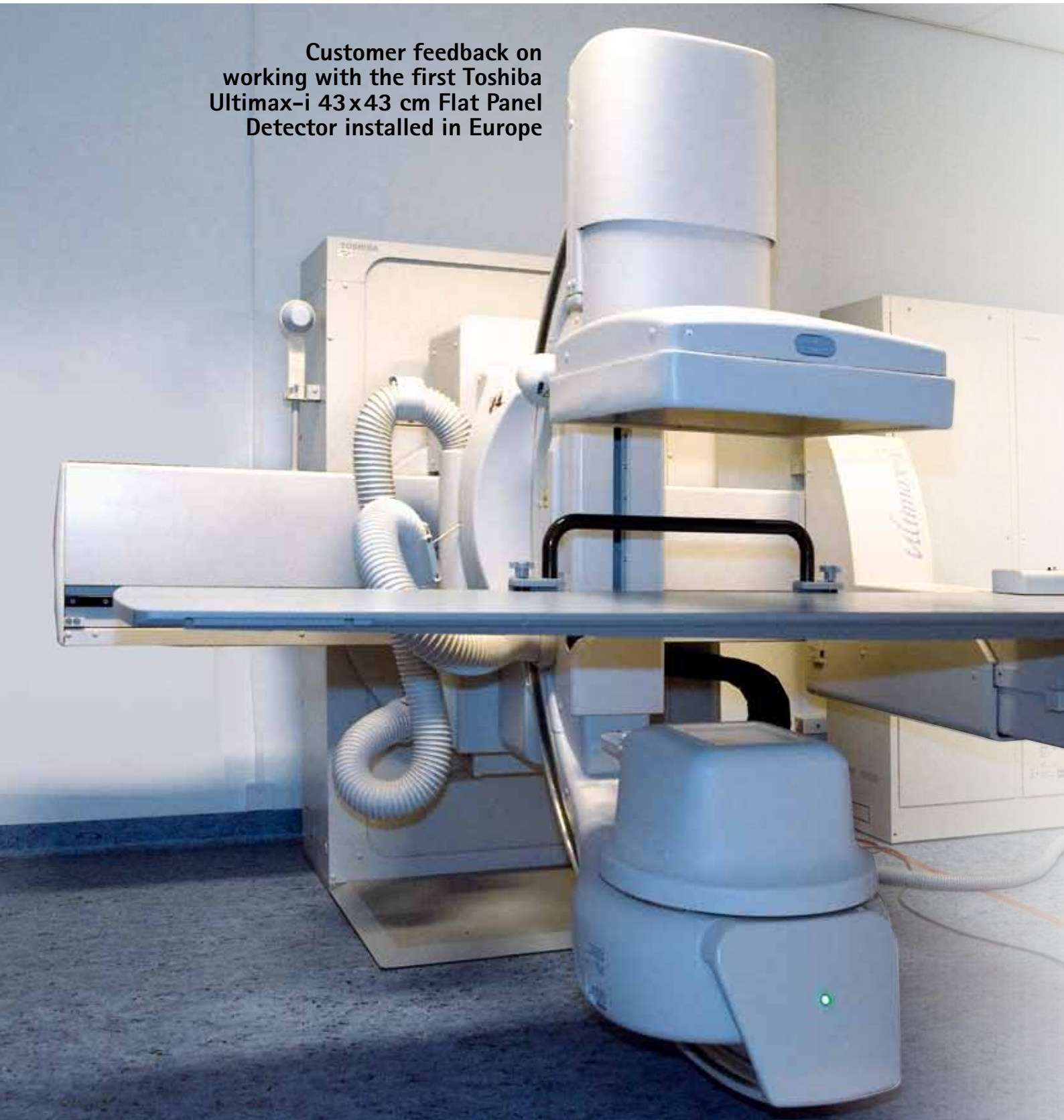

"It is a difficult job

to choose a new x-ray machine these days. Toshiba's Ultimax-i with 43x43 cm (17 inch) FPD offered a highly efficient solution."

Physicians all over Europe are opting for the high image quality, optimal versatility and efficiency and outstanding value offered by the Ultimax-i with 43x43 cm Flat Panel Detector (FPD), Toshiba's latest multipurpose x-ray system. More than 20 European orders have already been placed for the product since it was launched here last year. Featuring technology based on years of development at Toshiba, the system is proving ideal to meet the increasing diversity of needs in today's radiology department. Like all Toshiba products, it is designed with the challenges of the future in mind – making it a sound investment in the rapidly developing landscape of diagnostic imaging and interventional radiological therapy.

Dr JW Kuiper is a leading interventional radiologist at 't Langeland Hospital in Zoetermeer, the Netherlands, where the very first Ultimax-i with 43x43 cm FPD sold in Europe was installed in late summer last year. Visions talked to Dr. Kuiper about the history behind selection of the system and his initial experiences in working with it, nine months after its installation.

VISIONS: *Could you tell us about 't Langeland Hospital?*

Dr. Kuiper: This hospital serves the fast-growing city of Zoetermeer and surrounding towns in southwestern Netherlands. The city was really more like a small village until the late 1960s. It now covers an area of more than 37 km² and its population now tops 12,500, making it the third largest urban center in the province of South Holland, after Rotterdam and The Hague. 't Langeland hospital serves an even wider catchment area, with a total of 275,000 people. Over the next 15 years, it is anticipated that the population of the area will grow by another 30 percent. This will have a significant impact on the hospital's activities. In particular, the number of inhabitants in the area aged over 65 is expected to almost double from 27,000 to 53,000.

To provide extra facilities for the rapidly growing city, the hospital has recently undergone significant extension. Construction work was completed last year and we now have several new buildings providing extra facilities for eye health, rheumatology, pediatrics, neurology, internal medicine, urology and gynecology. There is a brand new dermatology department, dialysis center, senior health facility, Parkinson's disease clinic and sports clinic.

With extensive development of the hospital, we required new equipment and have also upgraded many older systems in order to maintain a high standard of care well into the future.

VISIONS: *Why did you choose the Ultimax-i from Toshiba?*

Dr Kuiper: The decision to choose the system from the many available ones involved a number of factors. I must say, it is a difficult job to choose a new x-ray machine these days.

The system had to deliver high-quality imaging across a very diverse range of clinical applications. The machine is used by five different radiologists here at 't Langeland, who work on a diverse range of scheduled and emergency cases. The workload includes interventional radiology, gastrointestinal studies and angiographic procedures. Toshiba's Ultimax-i with 17 inch FPD offered a highly efficient solution, enabling all these procedures to be carried out on one system in a single examination room. The system brings with it all the benefits of Flat Panel Detector technology together with a comprehensive dose reduction programme to provide a high-class versatile all-round system with excellent image quality, whatever the application.

The system's physical adaptability, rapid table and C-arm motion mean that virtually any position and projection can be obtained rapidly and smoothly when capturing clinical images. The anti-collision technology of the system protects the patient at all times.

While we have had a limited throughput of just 1,160 patients so far this year this is set to increase significantly in the future and so maximum

"The post-processing capabilities *of the Ultimax-i were also ideal for adaptation to our recently upgraded IT infrastructure."*

manoeuvrability will be essential in streamlining workflow in the future. The post-processing capabilities of the Ultimax-i were also ideal for adaptation to our recently upgraded IT infrastructure. Toshiba's excellent service package was an added attraction and last but by no means least the additional utility of the system was affordable.

VISIONS: *How was the installation of the system handled?*

Dr Kuiper: We ordered the system from Toshiba Medical Systems Europe in May 2009. Delivery took just three months - the system arrived in August and installation began right away. At the time, the hospital was still in the process of construction, but the new room for the Ultimax-i was ready. Toshiba's installation team ensured that we were well prepared to receive the new system. There are a number of important prerequisites which must be considered before installation of the system can start because of certain physical and operational features of this product.

With the new system, the table on the base unit can be lowered or lifted to give easier access for patients and it can also be tilted to an upright position. Extra space around the machine is important for ensuring easy access by the patient being examined and the healthcare professional carrying out clinical applications, such as interventional procedures and ERCP (Endoscopic Retrograde Cholangiopancreatography) examinations. However, from the broader perspective of spatial planning in the hospital it is actually space saving.

Different x-ray examinations can be performed in the same room because the system provides three systems in one. From a quality of care perspective this is also much better than transferring the patient between rooms for different examinations.

VISIONS: *Was learning to use the new system a challenge?*

Dr Kuiper: Not at all. Toshiba's experts individually trained each of the staff who will use the system in two weeks. Interacting with the system is so easy. The "one touch" master control enables minimal manual interaction with maximum automation.

Ultimax-i is the ideal solution for all patients as it combines three x-ray systems in one: angio, RF and DR

stration through purchasing, installation, training and operation. It has been a very rewarding experience. Toshiba's guidance has been invaluable. Delivery of the system was swift. The installation team has provided expert advice to ensure that every aspect of operation has been considered in setting up the system and integrating it seamlessly into daily use. And for the life of the machine, Toshiba continues to provide comprehensive technical support and applications.

What I particularly like is that Toshiba really listens to its customers and I am able to discuss further requirements, issues and areas for system improvement with all staff. The Dutch have a tendency to think about a product in terms of the benefits it provides to the individual – we think the product must fit us and not that we must adapt to the product. In that respect, we are perhaps some of the world's toughest customers to please! However, Toshiba has impressed me with the total package that it provides – outstanding product, excellent ongoing service and care and consideration for both the present and future in radiology.

VISIONS: *Thank you.*

VISIONS: *Which features of the Ultimax-i particularly impress you?*

Dr Kuiper: There are several features that are particularly beneficial to me as an interventional radiologist. The large Flat Panel Detector offers many benefits for image quality including lack of geometric distortion and improved ergonomics with better patient coverage. Moreover it enables dose reduction. I also really like the Super Noise Reduction Filter (SNRF) which enhances image quality significantly in fluoroscopy. I find the overall examination experience is improved with Toshiba's Ultimax-i silent, liquid-metal bearing x-ray tube. With the resultant lower ambient noise level, I can communicate more easily and effectively with staff members and patients.

VISIONS: *How do you rate the experience of working together with Toshiba on acquiring, installing and integrating the system?*

Dr Kuiper: In comparison to a larger, academic hospital such as the Erasmus Medical Center in Rotterdam where I worked previously, 't Langeland is a relatively quiet hospital. This has given me the opportunity to really interact with the whole Toshiba team from the initial investigation and demon-

"Different x-ray examinations *can be performed in the same room, because the system provides three systems in one."*

3D Wall Motion Tracking: implementing a new tool in daily clinical practice

A.S. Cerezo, L. Pérez de Isla, J. Rementería, W. Gorissen, J. Zamorano

Abstract

Since the introduction of ultrasound in cardio-logy, the wish to quantify cardiac function has been the driver for the development of new technologies. M-mode, which projects speckle information of cardiac structures over time, is so to speak the initial form of one-dimensional wall motion tracking. Two-dimensional speckle tracking is useful, has some limitations, though, because the heart has three dimensions. Now, the recently developed three-dimensional wall motion tracking (3D WMT) technology provides a new diagnostic tool. 3D WMT offers a new way to analyze the left ventricle and a new concept to assess its function. Moreover, it is not time-consuming and can thus be used as a routine analysis tool in daily clinical practice. 3D WMT is a new technique that can assess global and regional left ventricular (LV) function in a fast and comprehensive way. Its use may help the clinician to save time without having to make compromises in terms of completeness and accuracy of the analysis.

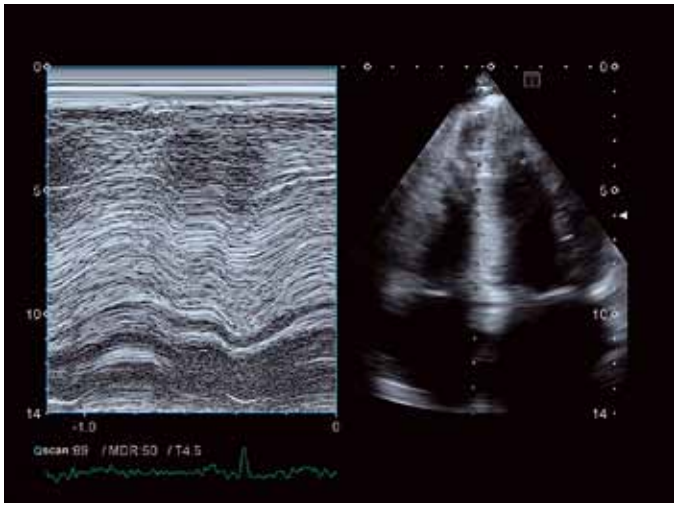

Fig. 1: Left ventricular septum M-mode shows how speckle moves with tissue.

Introduction

Traditionally, global left ventricular function has been evaluated using M-mode or two-dimensional (2D) echocardiography. More recently, three-dimensional (3D) echocardiography has been introduced in daily clinical practice. Segmental wall motion, however, has been difficult to assess. It is usually performed by measuring endocardium thickening, but this approach is limited by huge intraobserver and interobserver variability. Strain and strain-rate imaging have emerged as a quantitative technique to solve this problem[1]. Both measurements have been obtained from tissue Doppler imaging (TDI), but TDI-based strain and strain rate have several limitations: angle-dependent measurements (due to the use of Doppler) and simultaneous opposite deformation in the long and short axes[2]. A new technique called wall motion tracking (WMT) seems to solve the problem associated with TDI. The recent development of three-dimensional wall motion tracking (3D WMT) technology provides a new diagnostic tool: it is a fast new way to analyze the left ventricle and a new concept to assess left ventricular function.

Fig. 2: Left ventricular 2D WMT evaluation. The analysis of a short axis view is shown. The analysis of the whole left ventricle is very time-consuming.

Adriana Saltijeral Cerezo, MD[1], Leopoldo Pérez de Isla, MD, PhD, FESC[1], Juan Rementería[2], Willem Gorissen[2], José Zamorano, MD, PhD, FESC, EAE president[1].

[1]Unidad de Imagen Cardiovascular, Hospital Clínico San Carlos, Madrid, Spain
[2]Toshiba Medical Systems Europe

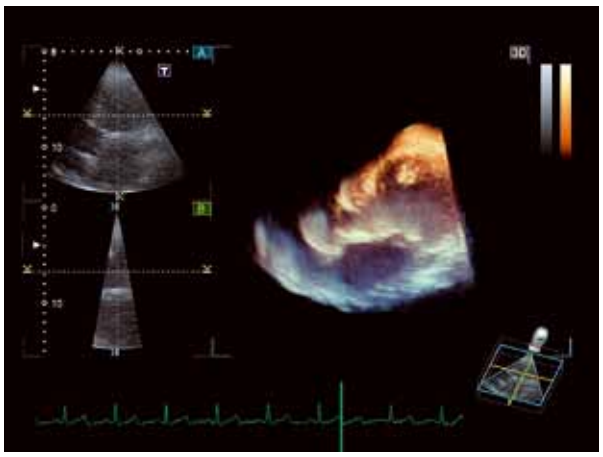

Fig. 3: 3D WMT detects speckle motion in three dimensions.

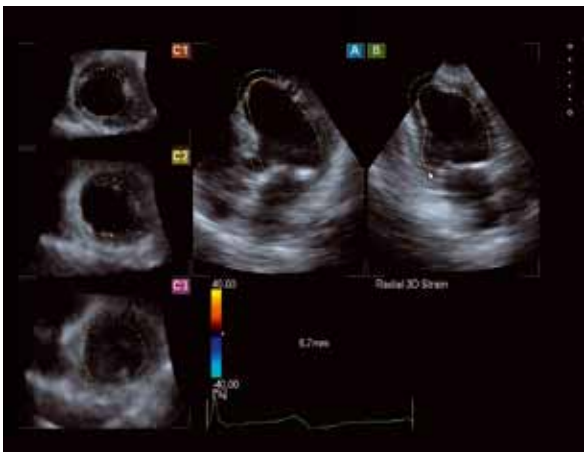

Fig. 4: Left ventricular semi-automatic tracking. The user sets three markers in planes A and B. The software detects the LV endocardium and the epicardium. See text for details.

Wall motion tracking

Speckle in ultrasound images is a phenomenon caused by interference of waves from randomly distributed scatterers in the myocardium. These scatterers are too small to be detected by ultrasound technology. Speckle degrades both spatial and contrast resolution by creating fine false structures, the so-called speckle noise. This phenomenon has a very important characteristic: speckle moves with the tissue. Thus, the speckle pattern follows the myocardial motion. Furthermore, each region of the myocardium shows a different speckle pattern due to the characteristic randomness of this phenomenon. Thus, a unique pattern is created for any selected region that can identify this region and the displacement of the region in the next frame. Motion is analyzed by integrating frame-to-frame changes[3]. Velocities can be calculated by the geometric shift of each speckle. The basic parameter of this information is displacement, and based on this value other parameters can be obtained[4,5,6]. Because M-mode projected the speckle information of the cardiac structures over time, it was so to speak the first form of one-dimensional speckle tracking (Fig. 1). One of the most important advantages of this method studied by Sivesgaard et al is the fact that there is no angle-dependency and multiple parameters can be calculated in different views[7].

2D wall motion tracking

Two-dimensional wall motion tracking (2D WMT) consists of a template image created using a local myocardial region in the starting frame of the image data. In the next frame an algorithm searches for the local speckle pattern that most closely matches the template. A movement vector is created using the location of the template and the matching pattern in the subsequent frame. Multiple templates are used to observe movement of the entire myocardium. The process is repeated by creating new templates and observing their movement in the subsequent frames until the entire cardiac cycle has been assessed.

Classically, strain and strain rate have been parameters obtained from tissue Doppler data[1].

Fig. 5a: A patient with hypertrophic cardiomyopathy. The type of display selected to present the results of the analysis of the left ventricular rotation is the so-called "plastic bag".

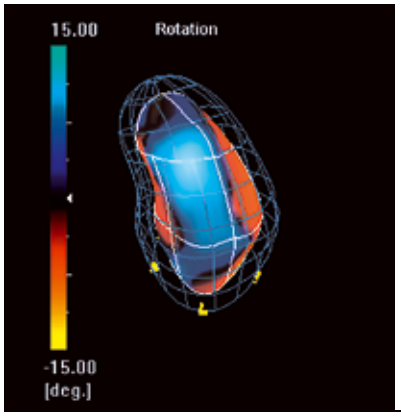

Fig. 5c: Polar map. Another way to present the 3D WMT results graphically.

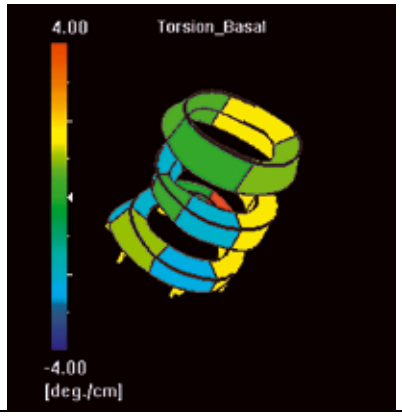

Fig. 5b: In this case, the selected parameter is the left ventricular torsion and the type of display chosen is the "doughnut view".

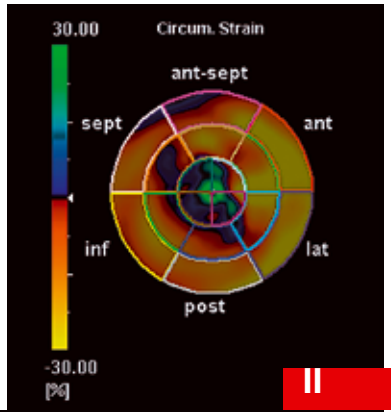

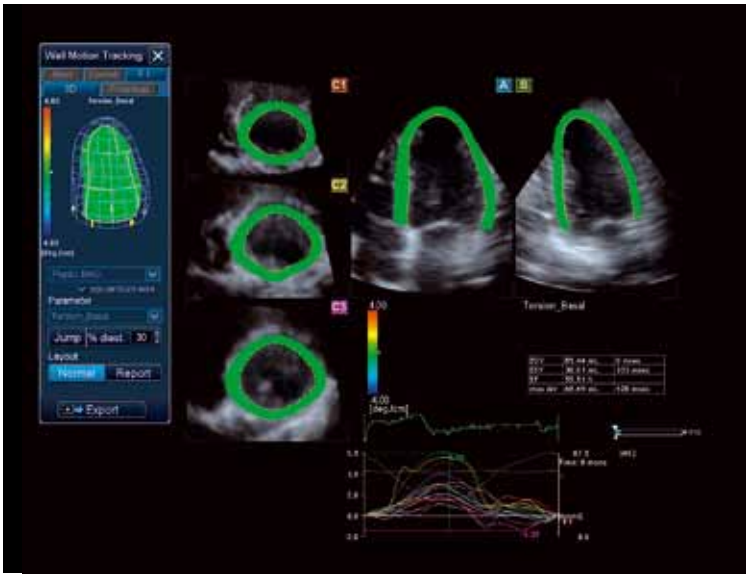

Fig. 6: Automatic calculation of left ventricular volumes and ejection fraction based on 3D WMT technology below the LV four-chamber view. The system automatically displays this information together with the wall analysis.

Nevertheless, WMT technology allows a new and more direct approach to obtain these parameters. 2D WMT can quantify regional myocardial deformation independently of insonation angle[7] and thus simultaneously assess long and short axis deformation. In this way, circumferential, radial and longitudinal strain can be obtained[2,8,9]. Furthermore, other parameters such as rotation, shear, twist and torsion may be evaluated (Fig. 2). WMT-derived strain and strain rate provide clinical relevant information in a huge number of cardiac diseases. Ingul et al analyzed patients with myocardial infarction and showed no difference between TDI and 2D WMT parameters in the infarcted area. Their results, however, showed that automated analysis methods were faster than and as accurate as manual analysis[10]. Seo et al studied thirty-three patients with severe symptomatic heart failure despite optimal pharmacologic therapy and showed that assessing left ventricle dyssynchrony using speckle tracking echocardiography results in a high rate of success for dyssynchrony assessment and clinically acceptable reproducibility[11]. Similar results were obtained by Delgado et al[12].

3D wall motion tracking

The heart has three dimensions. Cardiac motion is 3D and speckle noise moves in the three spatial directions. Thus, 2D WMT is limited because it cannot assess movement in the third dimension. The main difference between 2D and 3D WMT is that, although both techniques use ultrasound image data to detect movement of the myocardium, 2D WMT employs 2D movement or the projection of 3D movement into a 2D plane, whereas 3D tracking assesses real movement in 3D, not just a projection. 2D data is not used in this technique at any point. 3D WMT was developed as a new application that can be used for regional wall

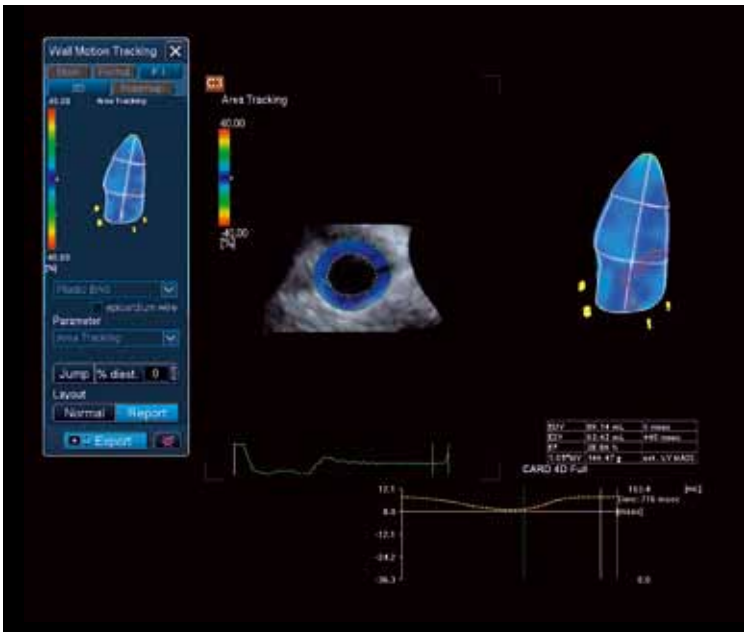

Fig. 7: Area tracking. A patient with ischemic cardiomyopathy and severely depressed left ventricular ejection fraction.

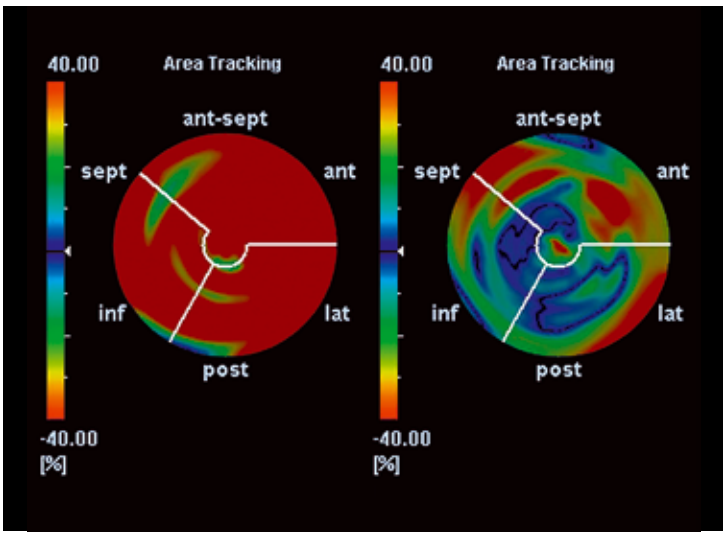

Fig. 8: On the left-hand side, area tracking of a patient without heart disease is shown and on the right-hand side, area tracking of a patient with severe ischemic heart disease is shown. The akinetic area is represented in blue.

motion analysis of the entire LV and allows to obtain real 3D indices and to assess 3D wall motion precisely with an improved integration of heart structures (Fig. 3). It is capable of displaying results for the entire myocardium using a single dataset to assess truly global LV. An overall dataset enables the user to observe new indices (e.g. torsion), true 3D strain and a host of other previously unobserved parameters[13].

3D speckle tracking has several advantages: all vectors of tissue tracking are tracked within the full volume. Moreover, lower volume rates can be used and it provides a better vector calculation which is more adequate for clinical scanning conditions and there is no loss of the speckle particle in 3D.

3D WMT requires the new Artida system and the PST-25SX 1 MHz to 4 MHz phased-array matrix transducer, both by Toshiba Medical Systems Corporation, Otawara, Japan. These two devices optimize 3D image acquisition. The matrix transducer can scan a user-selected volume that can be adjusted from 15°x15° to 90°x90°. For real-time purposes, one-beat acquisition is used and a triggered acquisition mode is available for advanced analyses. In the triggered mode (the mode used for 3D WMT evaluation), a live monitoring mode allows the user to monitor the reconstruction of the full-volume data set. The standard application setting is the use of four subvolumes of 90°x22.5°, which results in a 90°x90° triggered full volume in four heart cycles. During the acquisition, a five-plane view of the four- and two-chamber apical views and short axis planes at apex, mid and base of the LV is guiding the user to keep the best transducer position and updates the acquisition process continuously. During acquisition it is of great importance for the sub-volume to match well which can be monitored on the screen. If a mismatch appears, the examiner can continue the acquisition process until the mismatch disappears in the following heart cycles shown on the monitor. A retrospective acquisition method is used and after 'freeze' the best full-volume datasets can be selected from the image memory. A template for the B and C planes is available to set the right orientation of the A, B and C planes in order to achieve optimum plane selection.

Each 3D data set is displayed in a five-plane view: (A) an apical four-chamber view; (B) a second apical view orthogonal to plane A; and (C) three short-axis planes: plane C1 in the apical region, plane C2 in the mid-ventricle and plane C3 at the basal portion of the left ventricle. The user then sets three markers on planes A and B; in each plane, one marker is set at the apex and the other two at the edges of the mitral valve ring. The software then detects the LV endocardium, and the user sets a default thickness for the myocardium (Fig. 4). The software splits the LV into 16 segments automatically according to the American Heart Association standards for myocardial segmentation. After the markers have been selected, the system performs the 3D WMT analysis through the entire cardiac cycle. The selection of the LV shape is semiautomatic and the tracking process is automated, but the user can adjust the results of the tracking process if needed. Finally, the results of the 3D WMT analysis are presented as averaged values for each segment.

The 3D WMT analysis results can be displayed in different ways, such as the "plastic bag" (Fig. 5a), the "doughnuts view" (Fig. 5b) or the "dynamic polar map" (Fig. 5c) among others. The user can select from a wide variety of displays the one that shows the results most clearly. All these data may also be obtained in numeric format.

The new 3D WMT system works well with medium-quality echocardiography images. Saiko et al enrolled fifty-six healthy volunteers; ten subjects were excluded because of poor image quality[15]. In a study by our group thirty patients were analyzed and only two were excluded because of poor acoustic windows[14]. Furthermore, our results show how the 3D probe can obtain a more complete analysis, because the entire left ventricle may be analyzed from only one apical position and the sonographer does not need to change to different positions to obtain different planes. The 3D WMT technique is a simple, feasible and reproducible method to measure longitudinal, circumferential and radial strain values[15].

Time-saving is one of the main advantages of 3D WMT because all segments are calculated in one analysis step. Within 20 seconds, the result of 3D WMT is available with a large variety of parameters to read myocardial function. Different parameters

such as displacement and strain in longitudinal, radial and circumferential orientation are available in addition to the 3D vector-based variants. Moreover, new parameters such as twist and torsion are selectable based on rotation information which is also available as a display parameter.

Saiko et al and our group showed that inter-observer and intraobserver agreement for radial and longitudinal strain measurements on 3D WMT were good[14,15].

The 3D WMT analysis not only provides information regarding the segment analysis of the left ventricular myocardium, it also provides a robust evaluation of LV volume during the heart cycle. The detection of the endocardium for wall motion purpose is also useful to obtain the inner dimensions of the LV 3D shape and the myocardial volume. Thus, the system also provides information regarding LV volumes and LV ejection fraction and the related volume curves are presented time-aligned with the segmental parametric imaging curves. The detection of the endocardium is based on 3D tracking information and not on 2D plane assumptions. The 3D shapes can be corrected by the user when needed in five orthogonal planes. Thus, the assessment of the LV volume is anatomical correct and robust.

It results in a reproducible calculation of LV volumes and ejection fraction (Fig. 6).

3D WMT is a new tool which has demonstrated its usefulness in several clinical scenarios. It has a promising role in the evaluation of different heart diseases such as dilated cardiomyopathy, left ventricular asynchrony evaluation and ischemic heart disease[10].

3D WMT has a material limitation in time and spatial resolution. However, there was no significant difference in the time-to-peak strain between 3D WMT and 2D WMT. In addition, equivalent reproducibility of 3D WMT was demonstrated compared with 2D WMT[15].

3D WMT: exploring new parameters

Area tracking is a new parameter of regional and global LV function provided by 3D WMT on the Artida premium class ultrasound system from Toshiba Medical Systems. Area tracking reflects the 3D radial strain and is based on endocardial changes only, which makes the method very sensitive for detecting ischemic reactions in the myocardium which are most easily to recognize in the sub-endocardial layers (Fig. 7). This new method reflects the deformation of the endocardial surface during LV contraction and relaxation.

The application in combination with stress echo is a very promising tool to quantify stress echo readings. Area tracking facilitates detection of dyssynchrony and can be used in the selection of patients for cardiac resynchronization therapy (Fig. 8).

Conclusions

3D WMT is a new technique to assess global and regional left ventricular function quickly and comprehensively. It can help the clinician to save time without having to make compromises in terms of completeness and accuracy of the analysis.

3D WMT is a potential clinical bedside tool for quantifying global and regional left ventricular function.

New parameters such as area tracking with regard to screening and follow-up of patients with ischemic heart disease or dyssynchronous wall motion are being evaluated.

References
1 Marwick TH. Measurement of strain and strain rate by echocardiography: ready for prime time? J Am Coll Cardiol 2006; 47:1313-27.
2 Amundsen BH, Helle-Valle T, Edvardsen T, et al. Noninvasive myocardial strain measurement by speckle tracking echocardiography: validation against sonomicrometry and tagged magnetic resonance imaging. J Am Coll Cardiol 2006; 47:789-93.
3 Bohs L, Geiman B, Anderson M, Gebhart S, Trahey G. Speckle tracking for multi-dimensional flow estimation. Ultrasonics. 200; 38:369-75.
4 Bonnefous O, Pesque P. Time domain formulation of pulse-Doppler ultrasound and blood velocity estimation by crosscorrelation. Ultrason Imaging 1986; 8:73-85.
5 Trahey G, Hubbard S, von Ramm O. Angle-independent ultrasonic blood flow detection by frame-to-frame correlation of B-mode images. Ultrasonics 1988;26:271-6.
6 Perk G, Tunick PA, Kronzon I. Non-Doppler Two-dimensional Strain Imaging by Echocardiography: from Technical Considerations to Clinical Applications. J Am Soc Echocardiogr 2007; 20:234-43.
7 Kim Sivesgaard, MS, Sara Dahl Christensen, MSet al. Speckle Tracking Ultrasound Is Independent of Insonation Angle and Gain: An In Vitro Investigation of Agreement with Sonomicrometry J Am Soc Echocardiogr 2009; 22:852-858.
8 Leitman M, Lysyansky P, Sidenko S, et al. Two dimensional strain-a novel software for real-time quantitative echocardiographic assessment of myocardial function. J Am Soc Echocardiogr 2004; 17:1021-9.
9 Notomi Y, Lysyansky P, Setser RM, et al. Measurement of ventricular torsion by two-dimensional ultrasound speckle tracking imaging. J Am Coll Cardiol 2005; 45:2034-41.
10 Ingul CB, Torp H, Aase SA, et al. Automated analysis of strain rate and strain: feasibility and clinical applications. J Am Soc Echocardiogr 2005, 18:411-418.
11 Seo Y, Ishizu T et al. Mechanical Dyssynchrony Assessed by Speckle Tracking Imaging as a Reliable Predictor of Acute and Chronic Response to Cardiac Resynchronization Therapy. J Am Soc Echocardiogr 2009; 22:839-846.
12 Delgado V, Ypenburg C et al. Changes in Global Left Ventricular Function by Multidirectional Strain Assessment in Heart Failure Patients Undergoing Cardiac Resynchronization Therapy. J Am Soc Echocardiogr 2009; 22:688-694.
13 Pérez de Isla L, Vivas D, Zamorano J. Three-Dimensional Speckle Tracking. Current Cardiovascular Imaging Reports 2008, 1:25-29.
14 Pérez de Isla L, Balcones DV, Fernández-Golfín C, et al. Three-dimensional-wall motion tracking: a new and faster tool for myocardial strain assessment: comparison with two-dimensional-wallmotion tracking. J Am Soc Echocardiogr. 2009 Apr;22(4):325-30.
15 Ken Saito, MD, Hiroyuki Okura, MD et al. Comprehensive Evaluation of Left Ventricular Strain Using Speckle Tracking Echocardio-graphy in Normal Adults: Comparison of Three-Dimensional and Two-Dimensional Approaches. J Am Soc Echocardiogr 2009 2009 Sep 22-9: 1025-1030.

Abbreviations
2D = two-dimensional
WMT = wall motion tracking
2D WMT = 2D wall motion tracking
3D = three-dimensional
3D WMT = 3D wall motion tracking
LV = left ventricle
TDI = tissue Doppler imaging

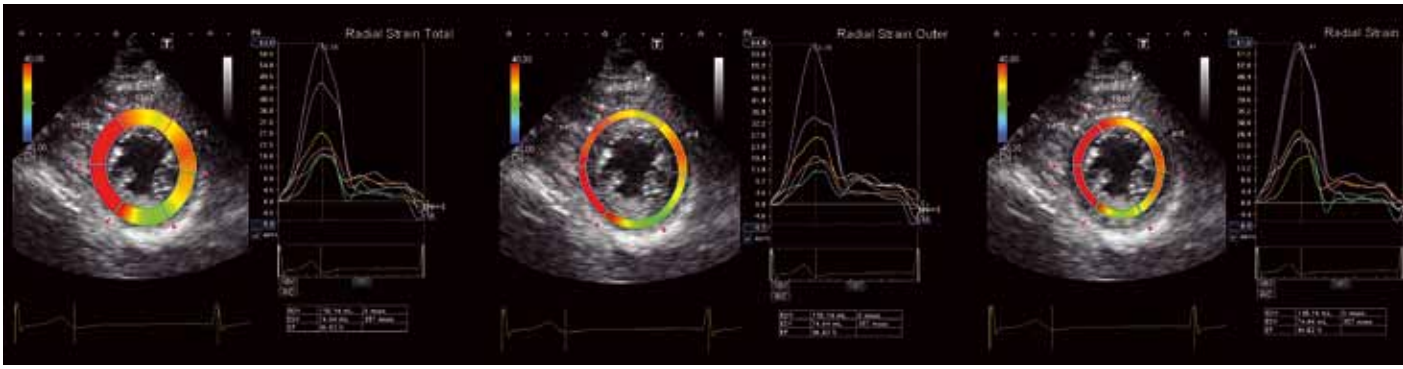

Advanced Multi-Layer Speckle Strain Permits Transmural Myocardial Function Analysis in Health and Disease

J.C. Hill[1], N. Mehta[2], G.P. Aurigemma[1]

Introduction

Two-dimensional (2D) speckle tracking echocardiography (STE) is now used to measure deformation and percent change (i.e. strain) in the myocardium for regional and global function. STE is based on conventional B-mode acoustic backscatter, permitting tracking of myocardial reflectivity (i.e. speckles) throughout the cardiac cycle[1]. Current STE methods measure the subendocardial-epicardial border interface, but do not permit analysis of deformation of the subepicardium or epicardium-to-endocardium. Recent advancements in STE by means of 2D wall motion tracking (2D WMT) have emerged allowing measurement of strain within layer-specific regions of the myocardium. This novel approach has been evaluated in normal subjects, patients with LV dysfunction and dyssynchrony, and validated against cardiac MRI in patients with non-transmural and transmural infarction[2,3]. The 2D-based STE multi-layer approach may provide further information on the heterogeneity of myocardial mechanics.

Here we present two cases. The first case is from a 41-year-old male with a history of hypertension who was referred to the echocardiography laboratory for evaluation of structural heart disease. The echocardiogram showed a left ventricular ejection fraction (LVEF) estimated in the range of 65–70% and no significant valvular disease. The second case is from a 61-year-old male with a history of ischemic cardiomyopathy. The echocardiogram showed normal left ventricular size with a LVEF estimated in the range of 40–45%. Findings included moderate hypokinesis of the inferior, basal-mid inferolateral, and entire septal wall. There was mild concentric hypertrophy and no significant valvular disease.

2D WMT speckle strain protocol

2D WMT was assessed in the parasternal short axis view at the papillary muscle level to obtain three-layer (inner, outer, total) radial strain analysis. Briefly, when acquiring images for 2D WMT, care is taken to optimize both the endocardial border and epicardial borders. Good image quality, on-axis imaging and acquisition during quiet respiration or apnea may improve tracking of the myocardium and reliability of data. To obtain 2D WMT, the online quantification program is accessed and the radial strain modality is chosen. The trace function is activated and four points along the LV endocardial border are chosen; a caliper is placed in a counter-clockwise direction at nine o'clock, six o'clock, three o'clock and twelve o'clock. The last point (twelve o'clock) automatically creates an epicardial border that is of equal distance from the endocardial border. The corresponding radial strain waveforms representing data from six myocardial segment are positive, and displayed above the baseline (Fig. 1). The processing time of 2D WMT from the point at which the raw data are obtained to strain results from each myocardial segment is roughly 35 to 40 seconds.

[1]*Jeffrey C Hill, BSC, RDCS; Gerard P Aurigemma, MD Echocardiography Laboratory, University of Massachusetts Memorial Healthcare and the Division of Cardiology, Department of Medicine, University of Massachusetts Medical School, Worcester, Massachusetts*

[2]*Nishaki Mehta, University of Massachusetts, Memorial Healthcare, Department of Medicine, University of Massachusetts Medical School, Worcester, Massachusetts*

Case 1: Normal multi-layer radial strain analysis

2D WMT radial strain demonstrated a layer-specific gradient across the myocardium during systole (Fig. 2). As predicted, the inner half subendocardial strains were normal and had the highest mean strain values, equalling 51% (Fig. 2a); there was a significant decrease in both regional and mean strains in the outer half, subepicardium equals 35% (Fig. 2b), with the total, mean transmural strains equal 43% (Fig. 2c). Of note, the majority of the radial strains from the corresponding segments peaked normally, occurring at the end of the T-wave on the ECG (i.e. aortic valve closure). These results demonstrate the uniformity in regional contraction and that a transmural gradient exists, with higher strain values in the subendocardial layer as confirmed previously by cardiac MRI[3].

Case 2: Abnormal multi-layer radial strain analysis

2D WMT radial strain failed to demonstrate layer-specific differences with significant heterogeneity in the peak strains (Fig. 3) which is in contrast to the normal findings. The majority of the inner half (subendocardial) strains were abnormal, with the lowest strain in the septal region equaling 18%. The mean inner half strain was abnormal, equaling 27% (Fig. 3a). Similar to the inner half subendocardial strains, the majority of the outer half subepicardium were abnormal with severe delay in the septal, inferior and posterior segments (arrows). The lowest strain was in the septal region, equaling 16%. There was no significant decrease in both regional and mean strain in the outer half subepicardium, equaling 28% (Fig. 3b). The total mean transmural strain equaled

Fig. 1a -e: 2D WMT speckle imaging protocol. The 2D image is frozen at end-systole and a caliper (arrow) is placed at the endocardial border at 9 o'clock, then located at 6 o'clock in a counterclockwise direction to activate the speckle tracking algorithm (a); the caliper is then indicated at 3 o'clock (b), then 12 o'clock (c). A double-click on the arrow creates an epicardial layer that is equally distanced (d). The image is then processed to create 6 equally spaced linear polygons with the corresponding radial strain waveforms shown in the extreme right panel (e).

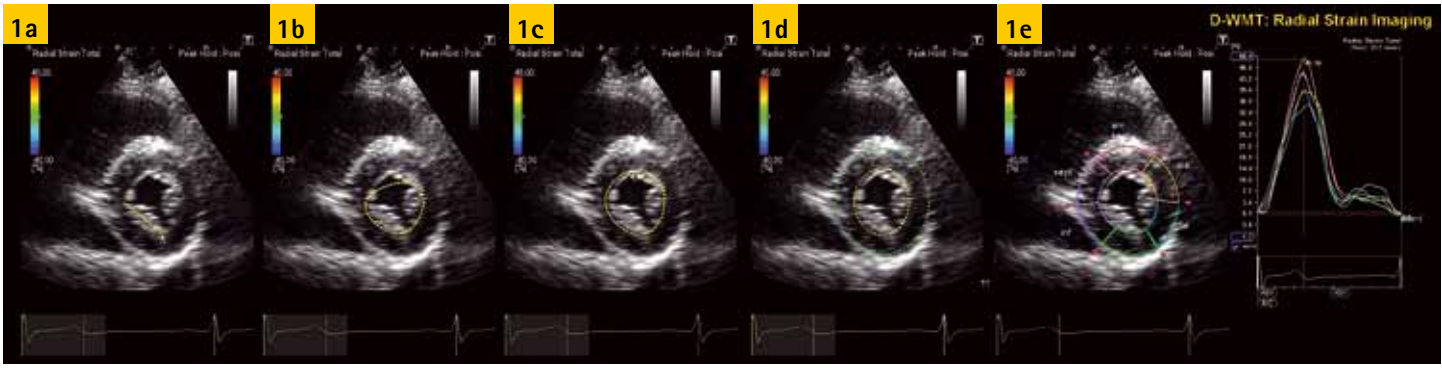

Fig. 2a-c: 2D WMT radial strain imaging in a patient with HTN and normal myocardial function. Mean subendocardial radial strain equals 51%, with the peaks occurring at end-systole at or near the end of the T-wave on the ECG (arrow). The vertical dotted line represents aortic valve closure (a). To the far right are the corresponding radial strain values from the 6 segment model; mean subepicardial radial strain equals 35% (b); mean transmural strain (average of both subepicardial and subendocardial strains) equals 43% (c).

Fig. 3a-c: 2D WMT radial strain imaging in a patient with ischemic cardiomyopathy and abnormal myocardial function. Mean subendocardial radial strain equals 27%, with a significant reduction and heterogeneity of the peaks (a); mean subepicardial radial strain equals 28% with significant delay in the septal, inferior and posterior regions (arrows) (b). This delay most likely represents active ischemia with late thickening occurring after aortic valve closure. Of note, the mean subepicardial strain gradients were greater than the subendocardial gradients; mean transmural strain (average of both subepicardial and subendocardial strains) equals 27% (c).

27% (Fig. 3c). These findings demonstrate no significant difference in strain at different layers of the myocardium with significant heterogeneity in peak strain.

Discussion

To elucidate the differences between heterogeneity and non-heterogeneity in the normal myocardium, radial strain or thickening is greater in the subendocardial layer than in the subepicardial layer. This transmural heterogeneity is explained by an increase in subendocardial wall stress, differences in myocardial blood flow, intramyocardial vascular resistance, myocardial metabolism and contraction and relaxation dynamics[4].

In abnormal myocardium, following periods of interrupted coronary blood flow, there is ischemia/necrosis that begins in the subendocardium and can extend through the ventricular wall resulting in transmural myocardial damage. This phenomenon is known as the "wavefront phenomenon"[5]. Furthermore, in the ischemic cascade, the subepicardial layer is reported to compensate for the decreased systolic thickening of the subendocardial layer which is referred to as "vertical compensation"[5]. This new multi-layer speckle strain approach for the evaluation of different layers of the myocardium may improve interpretation of regional wall motion. This technique can provide insight into pre-clinical changes in ischemia and other disease that may originate from the subendocardial regions.

Limitations

As with any ultrasound modality, the reliability and integrity of the data is highly predicated on 2D image quality. Newer ultrasound systems now have improved transducer technology which, when combined with harmonic imaging, can enable better visualization of myocardial structure and both endocardial and epicardial border definition. 2D frame rates for STE need to be between 40 and 80 frames per second (fps) in order to accurately characterize layer specific myocardial function. The average frame rate for the case studies was 74 fps.

Conclusion

Novel 2D WMT multi-layer speckle tracking was able to provide insights into regional differences in the myocardial deformation in both health and disease.

References
1 Hurlburt HM, Aurigemma GP, Hill JC, et al., Direct ultrasound measurement of longitudinal, circumferential, and radial strain using 2-dimensional strain imaging in normal adults. Echocardiography 2007;24:723-31.
2 Zhang Q, Fang F, Liang YJ, et al. A novel multi- layer approach of measuring myocardial strain and torsion by 2D speckle tracking imaging in normal subjects and patients with heart diseases, Int J Cardiol 2009, doi:10.1016/j.ijcard. 2009.07.041.
3 Becker M, Ocklenburg C, Altiok E, et al., Impact of infarct transmurality on layer-specific impairment of myocardial function: a myocardial deformation imaging study. Eur Heart J. 2009 Jun; 30(12):1467-76.
4 Kuwada Y, Takenaka K. Transmural heterogeneity of the left ventricular wall: subendocardial layer and subepicardial layer. J Cardiol. 2000 Mar;35(3):205-18.
5 Reimer KA, Jennings RB. The "wavefront phenomenon" of myocardial ischemic cell death. II. Transmural progression of necrosis within the framework of ischemic bed size (myocardium at risk) and collateral flow. Lab Invest. 1979 Jun;40(6):633-44.

3D Speckle Tracking

The diagnostic value of 3D wall motion tracking in the assessment of complex wall motion abnormalities

T. Wengenmayer

Introduction

Speckle tracking is a new technique that allows the reliable analysis of myocardial movement and deformation. Unlike tissue Doppler, speckle tracking is independent of cardiac translation and insonation angle as it is based on B-mode images. 3D speckle tracking evaluates strain, twist and rotation of the entire left-ventricular myocardium using a three-dimensional dataset. Before, the analysis relied on the sequential analysis of different two-dimensional views. With 3D speckle tracking the assessment of the total left-ventricular myocardium can be done with one capture. To evaluate the feasibility and accuracy of this new method we conducted a pilot study.

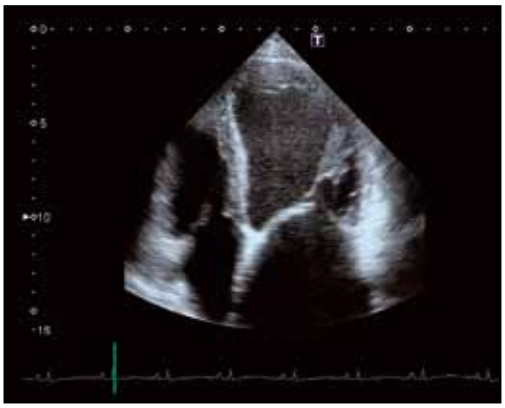

Fig. 1: Apical four-chamber view of a patient suffering from cardiac decompensation after heart transplant

In this study we examined a population of healthy volunteers and patients with different heart diseases. We would like to present a case of a young heart transplant patient. The patient presented with repeated cardiac decompensations accompanied by progressive weight gain and progressive dyspnoea. In 2001, the patient suffering from dilated cardio-myopathy underwent a heart transplant. Due to a CMV myocarditis and recurring, histologically confirmed rejection reactions, left-ventricular ejection fraction determined by echocardiography had been reduced but stable at approximately 30% for the past eight years. During the current hospital stay a conventional echocardio-graphy showed global reduced systolic left-ventricular function and severe hypokinesia – septal, anteroseptal and anterior. Ejection fraction was estimated by eyeballing to be 30% (Fig. 1).

As transversal or radial strain reflects myocardial contractility we assessed transversal strain of this patient. The two-dimensional analysis of transversal

Fig. 2: The automatic strain analysis in apical four-chamber view shows colour-coded transversal strain on the left. Strain curves for the 6 segments are displayed on the right. Yellow indicates preserved strain. Dark red indicates areas with reduced strain.

Fig. 3: The automatic strain analysis in apical three-chamber view shows colour-coded transversal strain on the left. Strain curves for the 6 segments are displayed on the right. Yellow indicates preserved strain. Dark red indicates areas with reduced strain. Blue indicates local dyskinesia.

Tobias Wengenmayer, MD
Department of Cardiology and Angiology
University of Freiburg, Germany

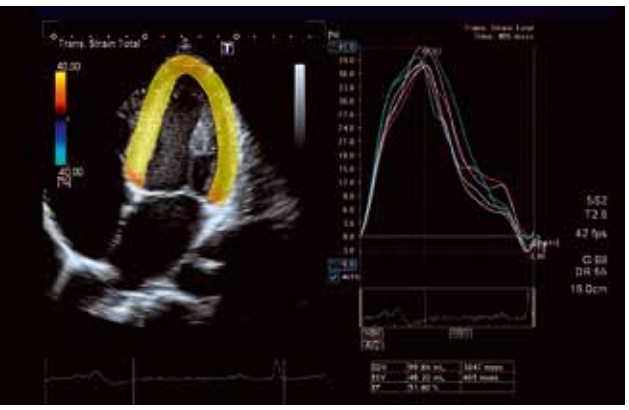

Fig. 4: Apical four-chamber view of a healthy volunteer. Colour-coding from yellow to blue indicates strain from + 40% to – 40%.

Fig. 5: Automatic strain analysis of the left ventricle. A short axis view from apex to basal segments (up to down) is shown on the left, four- and two-chamber views on the right. Bright yellow indicates preserved strain. Dark red indicates areas with reduced strain.

strain in four-chamber view confirmed reduced contractility of the septum as represented by the red coloured myocardium. The lateral wall showed a preserved transversal strain (Fig. 2). In the three-chamber view strain imaging showed reduced anteroseptal contractility with maximum strain values of 6% (Fig. 3) illustrating the reduced contractility. Based on the two-dimensional images a left-ventricular ejection fraction of approximately 32% percent was calculated. As an example for good left-ventricular contractility Figure 4 shows the four-chamber view of a healthy volunteer. Obviously contractility is preserved in all segments, as the homogenous colour-coding shows.

To quantify the complex wall motion abnormalities a 3D speckle tracking strain analysis was performed for this patient. Figure 5 shows the preserved radial strain from the apical lateral/inferior segments to the basal lateral segment whereas the rest of the left-ventricular myocardium shows reduced contractility. The left-ventricular ejection fraction based on the three-dimensional analysis was calculated to be 34.93%.

According to the reduced left-ventricular ejection fraction the maximal global radial strain (averaged radial strain of all segments) of the left ventricle was 11%. In healthy volunteers we found maximal global radial strain values to be around 30%.

We compared the echocardiographic data with MRI examination. With both methods the reduced global radial strain was obvious (Fig. 6).

As an example for the assessment of regional strain Figure 7 shows the radial strain of the posterior and septal segments. The red curves show echocardiographic, the blue curves show MRI measurements.

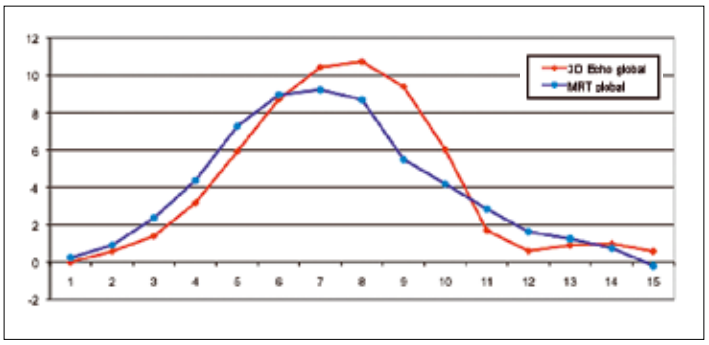

Fig. 6: Global radial strain measured with three-dimensional echocardiography and MRI. The red curve represents echocardiographic measurements, the blue curve MRI measurements.

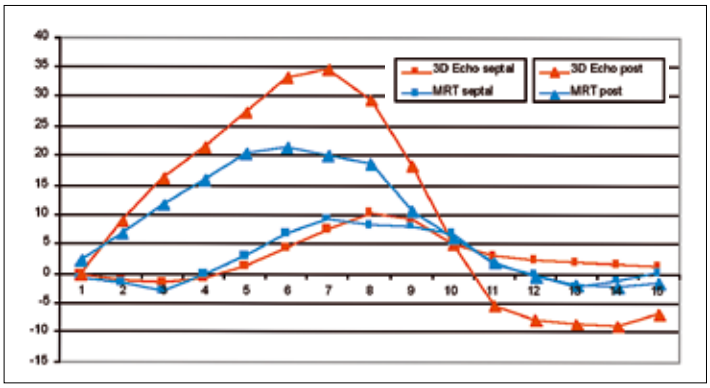

Fig. 7: Regional radial strain for septal and posterior segments. Red curves represent echocardiographic measurements, the blue curves MRI measurements. The triangle indicates posterior segments, whereas the square indicates septal segments.

Contractility in the extreme posterior segments of the myocardium was preserved, while septal contractility was visibly reduced. Moreover, maximum septal strain was reached earlier than maximum posterior strain. MRI showed generally lower radial strain rates. Both techniques showed a good correlation ($r > 0.9$).

Summary and conclusion

3D speckle tracking is well suited to capture, objectify and quantify wall movement abnormalities. Left-ventricular ejection fraction and global radial strain determined with 3D speckle tracking correlate strongly with MRI. 3D speckle tracking is a simple and fast bedside procedure. Radial strain provides good insights into myocardial contractility. The case presented here shows that this method provides a reliable and fast analysis also for patients with complex wall motion abnormalities.

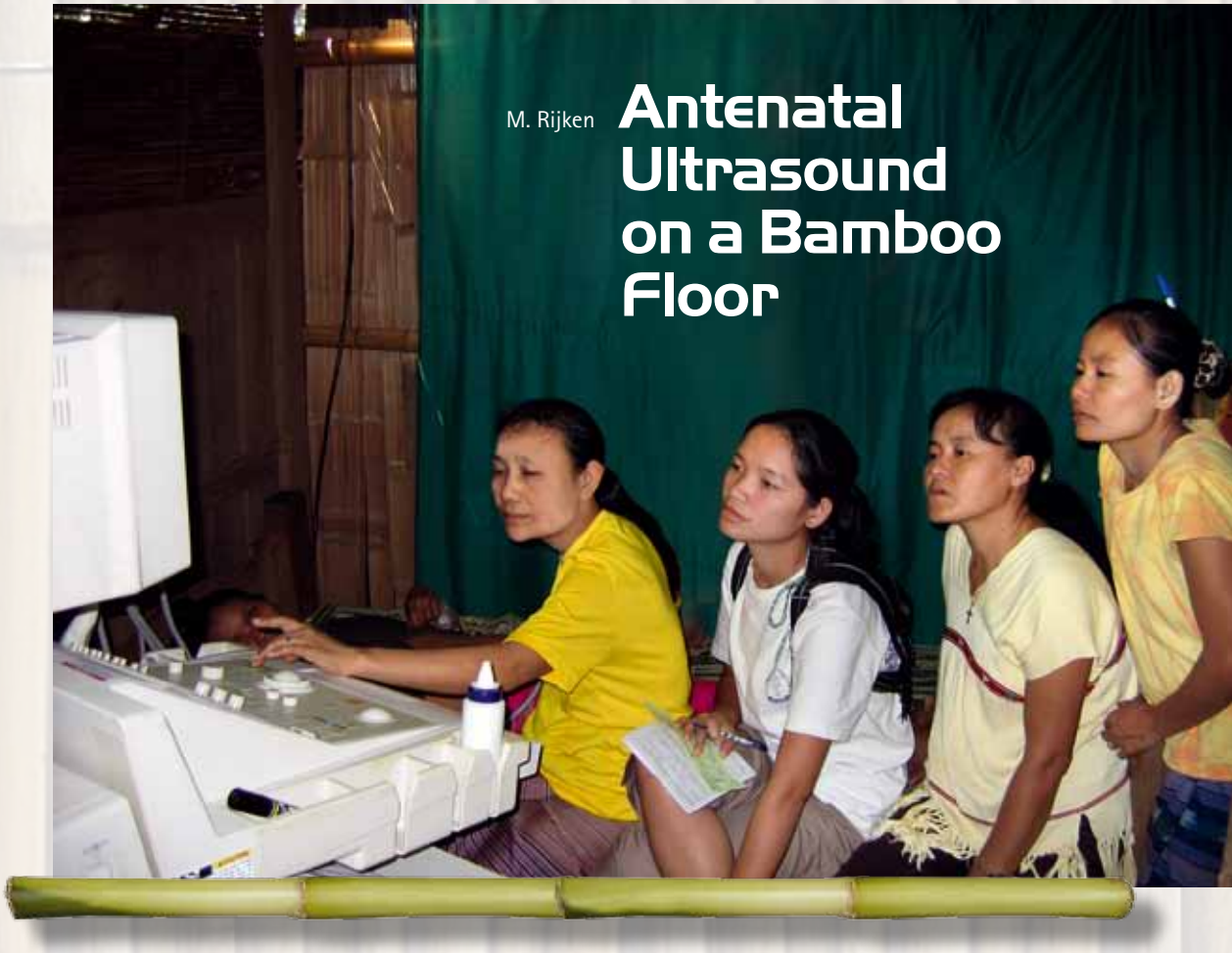

M. Rijken

Antenatal Ultrasound on a Bamboo Floor

Marcus Rijken, MD
Shoklo Malaria Research Unit Thailand

So much has changed. Twenty years ago, medical literature noted that "the use of ultrasound in developing countries is problematic because there are no machines or radiologists available." Meanwhile, it is inconceivable that in Western countries an OB/GYN clinic could function without ultrasound equipment. Even in primary antenatal care ultrasound has emerged as a valuable technology. Every woman in Europe receives at least one or two ultrasound scans during her pregnancy to determine for example the date of delivery and to monitor the fetus' health.

In Thailand, along the Burmese border, pregnant women are in need of the same kind of monitoring. They live under difficult circumstances and are at greater risk of complications in pregnancy, including infectious diseases such as malaria. The Shoklo Malaria Research Unit (SMRU, www.shoklo-unit.com) has five clinics along this border to provide assistance to migrants and refugees. In addition, the SMRU is investigating the optimal treatment of multi-resistant malaria in this area. The SMRU is a field station of the Tropical Medicine Department of the University of Oxford (UK) and Mahidol University, Bangkok. Together with my wife Machteld, I have been working in the SMRU since 2006.

Around 4,000 pregnant women a visit our ANC (Antenatal Clinics) each year. Half of these women cannot read or write, or both. No one knows exactly the date of their last menstruation. Here, women measure pregnancy duration in "waxing moons". What do we do in Europe if the pregnant woman's tummy is far too small? How do we determine how far along the pregnancy is? How can we tell if the baby is still alive? We use ultrasound. The same is true for heavily bleeding pregnant women, a threatening miscarriage, or an oversized tummy. Ultrasound technology has proved to play a vital role during pregnancy for many years. The SMRU believes that ultrasound in pregnancy can be very useful, ESPECIALLY in developing countries. For example pregnancy duration and location of the placenta are difficult to determine "manually" as is the assessment of multiple pregnancies. But this is vital information. Fortunately, the UMCU (University Medical Center Utrecht) and Toshiba agree! In 2006, they

donated a PowerVision plus box to transport the device from the Netherlands to Maela refugee camp on the Thai-Burmese border. At that time, Machteld and I had just started as doctors in the refugee camp and had begun conducting research on malaria in pregnancy. Three years later we have learnt so much. We have written about some of our experiences on the website www.malariadokters.nl.

The donated ultrasound machine is located in our hospital in the refugee camp on a bamboo wooden floor, under a canopy and has been in use every day for more than three years. Recently, Toshiba once again supported this project with a new transducer! Meanwhile, I have taught eight young women to make echoes and we are busy with a large study measuring fetal growth. Most of these local health workers have no medical training or experience; however, they are eager to learn and are very enthusiastic. After three months of training they sit an exam testing them on their ultrasound expertise. Our "Ultrasound Department" is professionally organized and there is always a doctor available for difficult cases. We have also established a continuous quality control system (intra- and inter-observer). Recently, we have published an article about these locally trained health workers as we found that they are able to carry out biometrics/growth scans of an adequate quality (see Rijken et al, Ultrasound Obstetrics Gynecology 2009; 34: 395-403).

Is ultrasound in developing countries a problem? In a well organized unit with continuous quality control and supervision, it is possible for locally trained staff to carry out good fetal growth scans. Expensive, highly trained radiologists are therefore not necessary. And the machines? They are becoming cheaper and more compact making it increasingly possible for ultrasound to be available in the developing world. In addition, old written-off machines from one of the many OB/GYN clinics in the West become available on a regular basis. Problematic? What we then need is people or companies prepared to give such a machine a "second life", in the jungle, on a bamboo wooden floor for example. Toshiba is one such company. Thank you!

Case Report

MR Imaging in Acute Marchiafava-Bignami Disease

A. Schiavello, D. Grisafi, C. Reina

Abstract

Various specific processes related to ethanol intoxication affect the CNS, as Wernicke encephalopathy, osmotic myelinolysis and Marchiafava-Bignami disease (MBD). Ethanol adversely affects vascular, glial and neural tissues and also causes myelin degeneration. MBD is an uncommon disorder associated with chronic alcoholism. This disorder was originally described in poorly nourished Italian men addicted to red wine consumption and it was first described by two Italian pathologists[1] who identified it in the autopsies of three patients who presented in status epilepticus and subsequently developed coma[2]. MBD has now been reported in other population groups and with various alcoholic beverages. MBD is characterized by primary demyelination of the corpus callosum and also by laminar cortical necrosis[3–8].

In this paper, we report a case of MBD in which MR imaging showed all the necrotic changes in the corpus callosum and in fronto-parietal grey matter. A 57-year-old male patient with a 30-year history of alcohol abuse (red wine) was brought to us in a state of mental confusion. He first showed gait disturbance and lack of motor coordination and then developed coma.

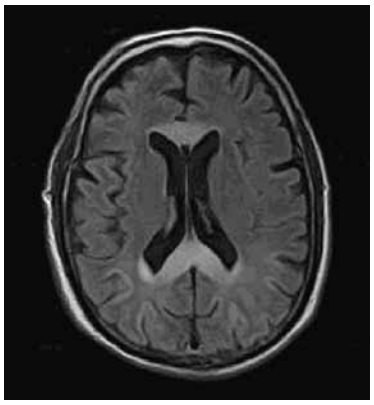

Fig. 1: Axial T2 FLAIR MR image showing an increased signal in the corpus callosum

Case report

Here we describe the clinical case of a 57-year old male patient with a 30-year history of alcohol abuse (red wine). Physical examination showed a malnourished individual with short- and long-term memory deficits, agraphia, impaired motor coordination, a wide-base gait, rigidity and overall diminished reflexes. The patient was examined using a 1.5 T superconducting MR scanner (Toshiba ExcelArt™). The MRI protocol included axial fast spin-echo T2-weighted sequences (TR/TE range, 4000–4900 ms /90–120ms); field of view [FOV], 18–22 × 22 cm; matrix, 160– 192 × 256–384; number of excitations [NEX], 1– 2; axial contrast enhanced spin-echo T1- weighted sequences (450–540 ms/10–15 ms; FOV, 18–22 × 22 cm; matrix, 160–176 × 258–384; NEX, 1– 2); axial FLAIR (fluid attenuation inversion recovery) sequences (8000–10000 ms/105–120 ms; FOV, 18 × 22; matrix, 160–192 × 256–320; NEX, 1–2; inversion time, 2,300–2,600 msec); and axial single-shot spin-echo echo-planar diffusion-weighted sequences with b values of 0 and 1000 s/mm^2 along all three orthogonal axes (4000–8000 ms/95–120ms; FOV, 22–25 × 26–30 cm; matrix, 128 × 128; NEX,[1]. FLAIR images showed increased signal intensity in the genu, the body and the anterior aspect of the corpus callosum (Fig 1). A moderatly increased signal of the occipital and parietal grey matter was noted (Fig 2). The diffusion-weighted images however clearly confirmed the increased signal in the isotropic b 1000 image in the corpus callosum as well as in the frontoparietal and in the temporo-parietal cerebral grey matter (Fig. 3 and Fig. 4). The patient was admitted and given intravenous vitamin B complex which resulted in a nearly complete settlement of the clinical manifestations of the disease.

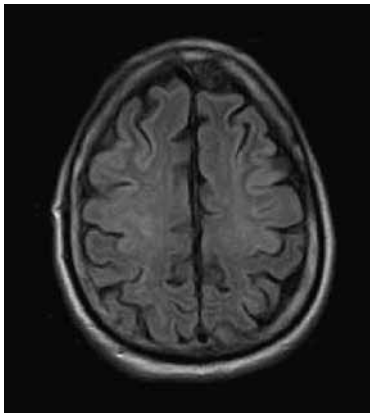

Fig. 2: Axial T2 FLAIR showing a weak and faded symmetrical hyperintense lesions in the occipito-parietal white matter

Discussion

MB disease or syndrome is a primary degeneration of the corpus callosum associated with chronic alcohol consumption but is occasionally seen in patients with no history of alcohol abuse. It is generally accepted that the

Alessandro Schiavello,
Domenico Grisafi,
Corrado Reina
Ospedale Buccheri
La Ferla, Palermo, Italy

disease is mainly due to a deficiency in the vitamin B complex. Although many patients improve following administration of these compounds, others do not, and in some patients the disease can be lethal. At first, MB was thought to be particular to individuals living in the central region of Italy and consuming large amounts of inexpensively manufactured Chianti red wine. It is now known that MB occurs worldwide and that all alcoholic beverages are implicated. Most patients are male, between 40 and 60 years of age and have a history of chronic alcoholism and malnutrition. The disease typically affects the body of the corpus callosum, followed by the genu and finally the splenium. The entire corpus callosum may also be involved. Other white matter tracts such as the anterior and posterior commisures and the cortico-spinal tracts may be involved. Lesions may also be found in the grey matter and in the middle cerebellar peduncles. The corpus callosum degenerates and splits into three layers ("layered necrosis"). Only the body or all of the corpus callosum may be affected. The necrosis leads to cystic cavities. During the acute phase of the disease, there are infiltrating macrophages but only a mild inflammatory reaction. The initial loss of myelin eventually gives rise to axonal loss. The reason the corpus callosum is affected is not known. Occasionally, the lateral putamina and the cortex are involved. Diagnosis is made on the basis of clinical findings in combination with imaging features. Patients present acutely with mental confusion, disorientation, neurocognitive deficits and seizures. Muscle rigidity and facial trismus may be severe. Most patients presenting with the acute type of MB will go into coma and eventually die, although as illustrated in this report, some survive. Acute MB may be difficult to distinguish from Wernicke encephalopathy and may coexist. Patients with Wernicke encephalopathy have ataxia, ophthalmoplegia, nystagmus and confusion. Patients with the subacute type of MB—which is characterized by dementia, disarthria and muscle hypertonia—may survive for years. The chronic form of MB is characterized by chronic dementia. In this latter form, the differential diagnosis includes Alzheimer disease, multi-infarct dementia and Pick disease. Also, chronic MB may have features similar to Korsakoff dementia. It is well known that rapid correction of the hyponatremia may lead to osmotic myelinolysis, and because 10% of all patients with pontine myelinolysis will have extrapontine lesions, some have suggested that MB may be yet another manifestation of the osmotic myelinolysis syndromes. On MR images, patients with MB show areas of low T1 signal intensity and high T2 and FLAIR signal intensity in the body of the corpus callosum at times extending into the genu and the adjacent white matter. These lesions do not have mass effect and may show peripheral contrast enhancement during the acute phase. Eventually, the lesions cavitate and become well marginated. The lesions are difficult to visualize on CT scans, where they appear as hypoattenuated areas. Other lesions involving the corpus callosum that may have a similar appearance include infarctions, shearing injuries and demyelination process. Tumors in this location generally have significant mass effect and contrast enhancement and are easily distinguished from MB. Differentiating acute MB from Wernicke encephalopathy is not difficult, because in the latter, MR imaging shows abnormal signal intensity and contrast enhancement in the mamillary bodies, periaqueductal region and the walls of the third ventricle. Acute pontine myelinolysis presents with abnormal T2 signal intensity in the base of the pons, and when extrapontine lesions are present, they generally involve the deep gray matter structures that are surrounded by white matter such as the basal ganglia. During the course of acute Marchiafava-Bignami disease, MR imaging is the appropriate technique to evaluate morphologic and metabolic changes of the corpus callosum, including their evolution over time and after treatment. DWI sequences may support the pathogenetic theory. The structural MR images may reveal a pathological condition only when this is associated to structural tissue damage. In our experience, DWI MR may integrate standard brain MR imaging, with reduced timing, making it possible to detect alterations which would remain unexposed by means of standard structural MR images.

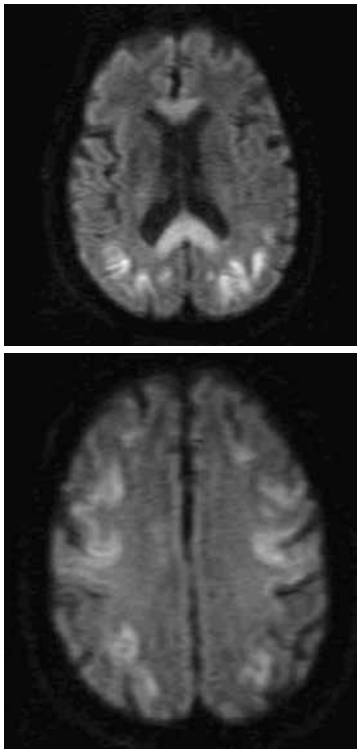

Fig. 3: Axial DWI (isotropic b 1000) MR image showing an increased signal in the temporo-occipital grey matter and involving the genu and the anterior aspect of the corpus callosum

Fig. 4 (below): Axial DWI MR image. The diffusion-weighted imaging (DWI) sequence shows abnorm increased signal intensity in the fronto-parietal grey matter due to laminar necrosis.

References

1 Navarro JF, Noriega S: Marchiafava Bignami disease. Rev Neurol 1999;28:519–523.
2 Victor M.: Persistent altered mentation due to ethanol. Neurol Clin 1993;11:639–661.
3 Marjama J, Yoshino MT, Reese C: Marchiafava-Bignami disease: premortem diagnosis of an acute case utilizing magnetic resonance imaging. J Neuroimaging 1994;4:106– 109.
4 Ishii K, Ikerjiri Y, Sasaki M: Regional cerebral glucose metabolism and blood flow in a patient with Marchiafava Bignami disease. Am J Neuroradiol 1999;20:1249–1251.
5 Girault JM, Armand JP, Dousset V, Daubé X, Schoenenberger P, Carller P, Caillé JM: Acute Marchiafava-Bignami disease: a case. J Radiol 1996;77:675–677.
6 Fortman BJ, Kuszyk BS: Incidentally diagnosed Marchiafava-Bignami disease. Am J Roentgenol 1999;173: 1713–1714.
7 Friese SA, Bitzer M, Freudenstein D, Voigt K, Küker W Classification of acquired lesions of the corpus callosum with MRI. Neuroradiology 2000;42:795–802.
8 Bourekas EC, Varakis K, Bruns D, Christoforidis GA, Baujan M, Slone HW, Kehagias D: Lesions of the corpus callosum: MR imaging and differential considerations in adults and children. Am J Roentgenol 2002; 179:251-257.

Toshiba's new president and CEO

Satoshi Tsunakawa

Former Senior Vice President Satoshi Tsunakawa has been appointed President and Chief Executive Officer of Toshiba Medical Systems Corporation, succeeding Kenichi Komatsu, PhD, who has become an adviser to the Toshiba Board.

Satoshi Tsunakawa, who joined the firm in 1979, has extensive experience in global sales, business and strategic planning. He has held positions at Toshiba's medical subsidiaries in Europe and the USA - where he was President of Toshiba America Medical Systems from 2004-2008.

For the past year, Mr Tsunakawa has led the global sales, strategic planning and corporate communications functions. "Toshiba has built a reputation as a leader in customer satisfaction," the new CEO pointed out. "We will continue to focus on being true partners with our customers worldwide by supporting and working with them as they strive to meet the challenges provided by today's quickly changing healthcare environment."

Congratulations! 25 years of PC innovations – and more

The 25th anniversary of Toshiba's production of portable PCs sees the launch of four more pioneering products:

The libretto W100 - the world's first dual touch-screen Windows mini-notebook PC – is pocket-size, weighs just 699 g and has distinctive dual 7.0-inch wide LCDs that offer a display equivalent to a 10-inch wide screen. The clamshell case opens like a book or notebook PC to reveal the world's first Windows platform to integrate dual touch-sensitive screens. Used as a PC, the libretto displays a haptic keyboard on the lower screen, but when held vertically it becomes an ebook reader displaying a double-page spread.

The dynabook RX3 is the world's lightest 13.3-inch wide LCD display laptop. Weighing in at just 1.25 kg, due to the highly durable honeycomb-structured chassis, and despite its slim lines, the notebook integrates an optical disk drive, standard voltage CPU and a battery with a maximum life of about 11 hours.

The dynabook Qosmio DX is an all-in-one AV PC that offers a full HD 21.5-inch wide LCD display and the world's fastest write times to Blu-ray discs. The display of this stylish, space-saving, all-in-one AV-PC is special, not least due to its Toshiba Quad Core HD Processor SpursEngine – a dedicated image processor with advanced performance derived from the multi-core technology of the Cell Broadband Engine.

The SpursEngine boosts recording density, enabling about 1,048 hours of terrestrial digital programmes to be recorded – eight times as long as when recorded in the original density. Another unique capability is its Super Resolution Technology which upscales SD video sources, e.g. camcorder videos, to near full HD picture quality to use on-screen or save to Blu-ray discs.

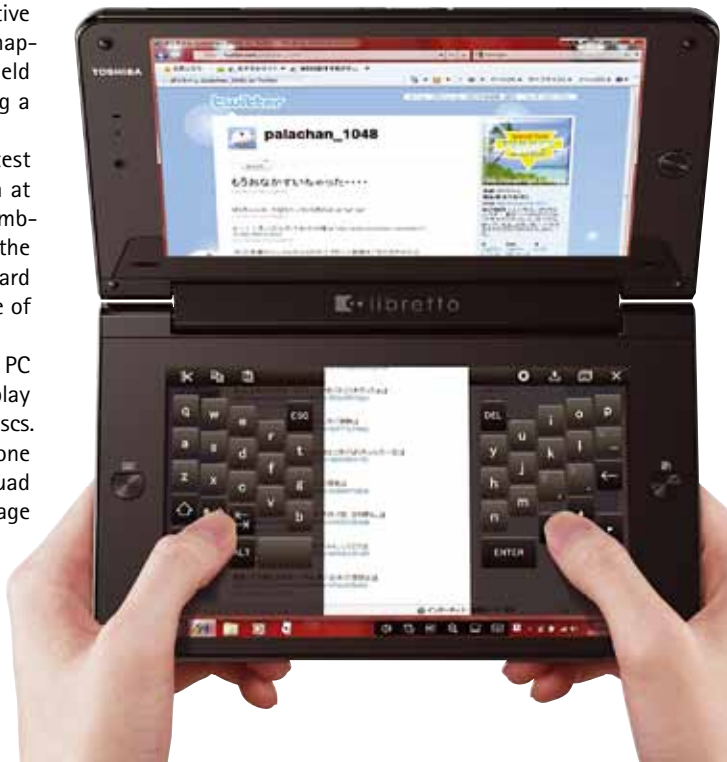

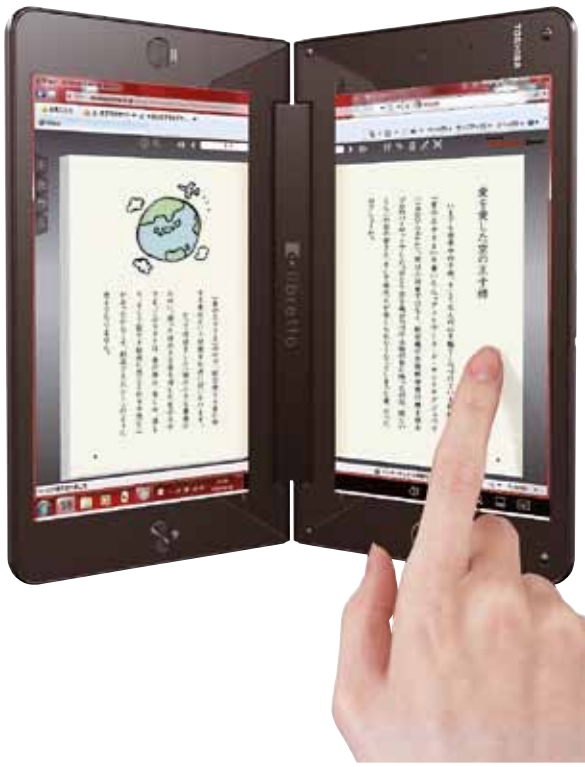

Toshiba's advanced power management technology endows this device with a level of energy efficiency rare in an all-in-one PC, which earned the dynabook Quosmio DX the Green Mark (awarded to products that meet the Japanese standard for energy saving).

The dynabook AZ is always on and internet-ready, an ultraslim 'cloudbook' that weighs just 870 g and yet provides users with all they need. It is world-wide the first clam-shell type net-work device to integrate the NVIDIA TegraTM250 Processor, a 10.1-inch wide LCD with LED backlighting and the full-size keyboard of a netbook on the AndroidTM 2.1 platform. With the dynabook AZ, Toshiba has combined the best of two product categories: the operability, large screen and full-size keyboard of a PC, with instant start-up and power consumption similar to a smartphone, enabling it to remain on standby for up to 180 hours. Adoption of the NVIDIA TegraTM250 Processor and an HDMI output realizes outstanding AV performance, including connection to an HDTV for display of HD content.

We take care – CSR Report 2010

The new edition of the Toshiba Group Corporate Social Responsibility Report 2010, a comprehensive account of the Group's latest CSR activities, has just been published.

The CSR Report 2010 provides the stakeholders with an authoritative resource on the company's CSR policies, plans, programs and activities. This year's Report mainly features two special reports: the Integrity Report I features the company's initiatives in business activities that contribute to protection of the global environment, and Integrity Report II presents selected information in accordance with the international standards (seven core subjects of ISO 26000 Draft International Standard) and guidelines for CSR reporting. The key contents of the Reports are as follows:

Integrity Report I

- Vision and goals of Toshiba Group in establishing itself as one of the world's foremost eco-companies, and related initiatives
- Environmental Vision 2050 addresses environmental challenges
- 1 Greening of Process
- 2 Greening of Products
- 3 Greening by Technology

Integrity Report II

- CSR Reporting Policy
- Organizational Governance
- Human Rights
- Labor Practices
- The Environment
- Fair Operating Practices
- Customers
- Community Involvement and Development

For more information and download of the CSR report
http://www.toshiba.co.jp/csr/en/engagement/report/index.htm

Entering the Wi-Fi SD card arena

Toshiba and Singapore-based Trek 2000 International Limited have founded the Standard Promotion Forum for Memory Cards Embedding Wireless LAN to promote a new SD card that integrates Wi-Fi wireless communication with data storage capabilities.

In recent years, as digital cameras have achieved huge rates of market penetration, the need for a quick, easy way to share photographs has increased. The new card presents new capabilities to the already popular SDHC format by bringing Wi-Fi functionality to digital still cameras with an SDHC slot. Once in a camera, a card can recognize and communicate with the same type of card in another camera, so that users can exchange photographs quickly and easily. Uploading and downloading images to and from a server without a cable connection or transfers of the memory card is no longer a problem.

The new 8 GB card is compliant with the SD memory card standard. It can transfer JPEG and RAW images, the two most widely used digital formats.

Toshiba and Trek will invite the participation of digital camera manufacturers and other interested parties in promoting the card and exchanges of technical information toward establishing standard specifications and expanding the use of the card.

Nuclear power talks

TerraPower, a company owned by Microsoft chairman Bill Gates, is in preliminary discussions with Toshiba regarding a new generation of nuclear reactors.

Both firms are investigating technology for mini-reactors, which are more cost-efficient than conventional units, in the hope that they might be suitable for use in cities or emerging world markets.

Called Travelling-Wave Reactors (TWR), the new technology promises nuclear reactors that can operate for 100 years without refuelling, unlike today's units that need replenishment every few years.

Last year, Bill Gates visited the Toshiba laboratory for nuclear power research, near Tokyo, to discuss the project.

Keisuke Ohmori, a Toshiba spokesman, confirmed that Toshiba and TerraPower "are looking into the possibility of working together" and have begun to "exchange information" but that "nothing concrete has been decided on development or investment".

Rugby – Toshiba to tackle World Cup sponsorship

The Toshiba Corporation has been selected as an Official Sponsor of the Rugby World Cup 2011, to be held in New Zealand next year (9 September to 23 October).

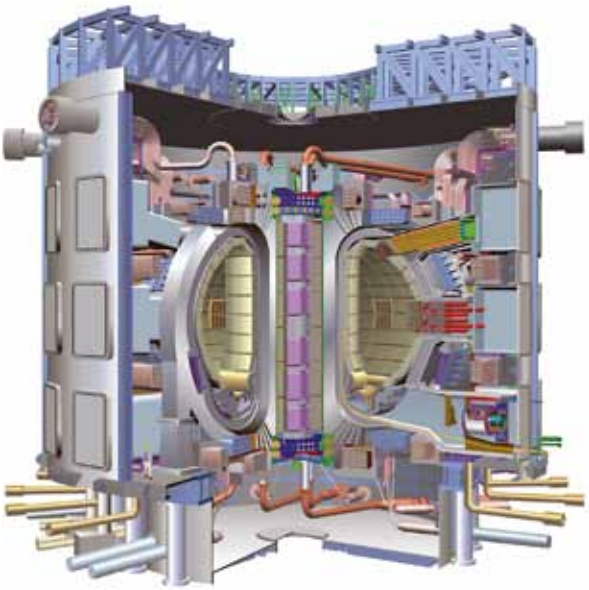

Since its inauguration in 1987, the quadrennial Rugby World Cup has become one of the biggest events in the global sporting calendar. France 2007 attracted more than two million spectators and was viewed by a cumulative global TV audience of 4.3 billion concentrated in Europe, Oceania and Asia. Rugby World Cup 2011 is expected to deliver an irresistible mix of world class rugby with impressive venues. This, the 7th Rugby World Cup, will be the largest sporting competition ever held in New Zealand. Around 70,000 overseas visitors are expected to attend the games, whilst billions more will watch on-screen broadcasts worldwide.

Toshiba has a notably long association with rugby and cultivation of the game in Japan. Brave Lupus, the firm's own rugby team, competes in Ja-

pan's Rugby Top League and has sent numerous players for Japan's national team in the six Rugby World Cup Tournaments. Additionally, in 2007, the company sponsored the Rugby World Cup in France.

Toshiba's sponsorship is not only an opportunity to support rugby but also to spotlight its products – the firm will provide, for example, TVs and Blu-ray disc players, notebook PCs and digital multi-function peripherals integrating a copier, printer, scanner and network capabilities, as well as air-conditioning equipment.

The company will run a rugby-themed advertising campaign that will include advertising signage in the stadiums, incorporated tournament logos in its product and corporate advertisements, and banner ads on the official Rugby World Cup 2011 website. "We are very much looking forward to building on the success of our sponsorship of Rugby World Cup 2007," said Mark Whittard, Managing Director, Toshiba (Australia) Pty Ltd.

Equally pleased is International Rugby Board Chairman, Bernard Lapasset, who added that Rugby World Cup Limited is delighted that Toshiba has joined the impressive list of sponsors for Rugby World Cup 2011: "The re-appointment of a world leader in the electronics field further underlines the enormous attraction and prestige of the tournament in the global sporting calendar."

LEDs to light up the Louvre

Paris, France: Toshiba's state-of-the-art LED lighting will soon illuminate some of the Louvre museum's most visited public spaces.

In a lighting renovations project, the Louvre, one of the world's most eminent museums, plans to replace energy consuming xenon lighting with an environmentally friendly solution. Toshiba will provide its energy saving low-CO2 LED lighting products to illuminate some of the museum's most familiar spaces: the Pyramids that greet visitors as they approach the museum, the Napoléon Court and the Cour carrée, the main entrance to the museum.

Beyond environmental concerns, the Louvre needs lighting that conveys the intrinsic beauty and spirit of a museum that is home to some of the world's greatest art. Toshiba points out that lighting is far more than a means to brighten public spaces, and LED lighting can contribute much more than energy saving. The defining theme of Toshiba's lighting is akari, which in a pre-modern era often meant candlelight, an essential part of life. Today, akari is a Japanese concept that conveys the ability of lighting to appeal deeply to our senses and emotions.

Electric bicycles powered by rechargeable batteries

Shimano Inc., the world's largest manufacturer of bicycle parts, has selected the SCiB™ battery for the power module of a battery system for electric bicycles that Shimano supplies as a component to bicycle manufacturers. The new power generating device is Toshiba's breakthrough rechargeable lithium-ion battery that combines long life and rapid recharging with high-level regenerative charging, characteristics that make it highly suited to application in electric bicycles.

The battery module will integrate SCiB cells and a battery management system that optimizes use of the SCiB's characteristics by monitoring the energy use during operation and charging and protects the cells. It also supports regenerative charging of electricity from energy generated while braking or coasting downhill. High mileage will be achieved by combining the cell's rapid recharging and excellent regenerative capability with the Shimano motor and inverter system with highly efficient regenerative function. The SCiB's long life will also promote reduction in waste from battery replacement and contribute to a society that saves energy and reduces environmental loads.

The battery module will be installed in a new product that Shimano is scheduled to supply to the European electric bicycle market by the end of this year.

Aquilion CX allows for medical examination of large zoo animals.

Wild animals under a CT scanner

In the future, the Leibniz-Institut für Zoo- und Wildtierforschung (IZW) in Berlin will use the Aquilion CX by Toshiba Medical Systems to examine sick animals. With its 72 cm bore, which can accommodate even baby elephants, and the heavy-load table for up to 300 kg the CT scanner was designed especially for veterinary medicine.

In Berlin, the Aquilion CX will for the first time be used with large animals. The machine produces 128 images of various layers of the body with a single gantry rotation. In only half a minute it can generate more than 4,000 slices. The 2D images are then converted into 3D images. The huge computational effort is justified: the researchers are able to see structures of only half a millimetre.

One of the first tests of the CT scanner was the examination of a six months old female elephant, Jamuna Toni, from the zoo in Munich. Unfortunately, the young animal had to be put down, because it could no longer move. The CT confirmed the zoo team's suspicion: Jamuna Toni had been suffering from a malignant and incurable bone disease. Thomas Hildebrandt, head of IZW, and his team, however, intend to use the Aquilion CX primarily for examinations of living animals. The high-performance CT is also a valuable tool for prophylactic purposes, for example with regard to giraffes that in captivity tend to develop inflammations at the claws. "Maybe we will also be able to learn how hippopotami communicate under water," says Hildebrandt. Since deep sounds are carried very far under water, marine mammals communicate in extremely low frequencies. The animals develop calcium structures in the inner ear that improve hearing. Since these filigree structures are difficult to examine in the skulls of dead animals, the scientists want to use the CT to look for them in the inner ears of living hippopotami. If present, these structures would explain the animals' good infrasound perception.

TOSHIBA

Leading Innovation

Aquilion ONE

Complete your myocardial diagnosis in just ONE examination

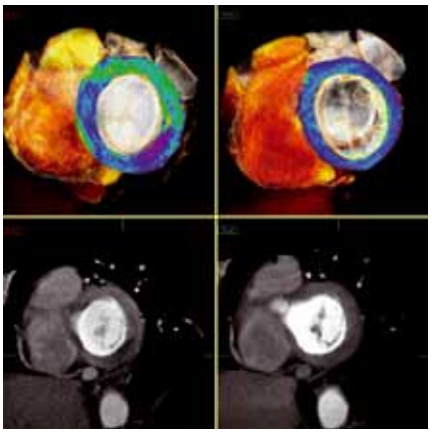

Myocardial Perfusion study made by Toshiba's Aquilion ONE

The unique ability of Aquilion ONE to acquire the entire heart in a single temporally uniform volume permits quantitative myocardial perfusion analysis to be performed with the same data used for coronary CTA. A similar acquisition during pharmacological stress permits the comprehensive evaluation of myocardial perfusion in ONE examination.

Comprehensive functional and morphological cardiac analysis with Aquilion ONE can reduce the need to perform multiple examinations using different modalities which saves you time, money and minimizes the total patient radiation dose!

Toshiba: Made for Patients, Made for You, Made for Partnership!

Made for Life™

www.toshiba-medical.eu

ULTRASOUND CT MRI X-RAY SERVICES

Re-engineering the Patient Pathway

Introducing Aquilion ONE into an emergency department can shorten time to diagnosis for chest pain patients and decrease the costs of hospitalization

Computed tomography (CT) is now considered sufficiently robust and reliable to be used routinely for patients presenting with chest pain, a common symptom accounting for approximately 6% of hospital emergencies.

While many of these cases prove to be minor, the potential for serious and life-threatening conditions means that the majority of patients need to undergo a series of costly and time-consuming diagnostic tests.

For example, a recent study[1] applying economic value modelling to the patient pathways at hospital trusts in the United Kingdom showed that around 70% of all chest pain patients are referred to Acute Medical Unit (AMU) for diagnosis during a short stay estimated to cost € 657.

Around 14% of all patients are transferred to an inpatient unit at the hospital for a definitive diagnosis with the time to diagnosis averaging three days at a cost of € 1,166.

The introduction of the Aquilion ONE from Toshiba presents a potential to change this traditional emergency patient pathway with a wide array of detectors for whole-heart data acquisition using low radiation dose techniques that enable a definitive diagnosis of chest pain patients in one protocol in a matter of minutes.

The study by Simon-Kucher & Partners examined detailed economic value modelling of the pathways in a large National Health Service Acute Trust and concluded the potential for cost reductions range from € 375,000 to € 1.8 million per year depending on the system's usage within the emergency department and the release capacity in the acute medical unit.

A decision tree model was developed to compare the current standard diagnostic pathway with a pathway using the Aquilion ONE to diagnose patients with acute chest pain.

The final node of each of these pathways is either the ultimate diagnosis of Acute Coronary Syndrome (ACS) or the exclusion of ACS, and for each final node the probability, associated cost and associated time spent on a ward were calculated and used to derive the overall cost of the patient-pathway

The current pathway was derived in close co-operation with one large NHS Acute Hospital Trust in the UK that sees 8,000 patients each year with acute chest pain and the study is based on discussions and analyses of patient files.

As the hospital did not use Aquilion ONE, the new pathway reflects the impact of this new CT scanner, and based on discussions with cardiologists and radiologists of four other NHS acute trusts and a review of literature the study's authors were able to

Dynamic volume scanner as the state-of-the-art scanner with its wide coverage provided by 16 cm-wide detector enables scanning of most of the organs with single, non helical rotation.

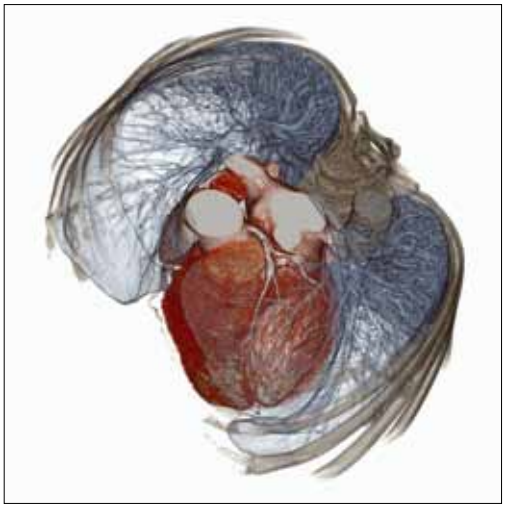

3D CTA dataset acquired by AquilionONE with single, non-helical rotation.

create a diagnostic pathway representative of other hospitals in the UK where a more usual number for an average size regional NHS Acute Trust would be 4,000 patients per annum.

Toshiba's Aquilion ONE has unique features that make it highly suitable for integration in the diagnostic pathway of patients with acute chest pain:

Aquilion ONE offers a clearly higher accuracy than currently available cardiac CT scanners even in the presence of irregular heart rates.

With 16 cm coverage in one rotation it is capable of perforrming whole organ scans in a sub-second, offering dynamic volume imaging with a single, non-helical rotation.

Because data are typically acquired in a fraction of a second during a single heart beat, the entire 3D dataset is temporally uniform and not constructed from multiple consecutive heart beats as with scanners with fewer detector rows, thereby reducing heart rate- and breathing-related motion artifacts and increasing image quality.

The Aquilion ONE also uses a radiation dose below those of conventional scanners and less contrast media for prospective CTA examinations.

Data was retrospectively collected for 62 patients who presented to the high-volume hospital trust and the analysis of the resource consumption focused on the main cost drivers, which are the level of emergency service, number of AMU days, number of inpatient days and the cost of an Aquilion ONE scan.

The comparison of the patient pathway using Aquilion ONE against the traditional pathway revealed that Aquilion ONE allows for an ultimate diagnosis for all patients in Emergency. This results in a release of capacities on AMU and inpatient units as well as cost savings for the hospital.

For 4,000 patients presenting each year to Emergency with acute chest pain, the hospital investigated had the potential to save around 2,400 AMU days and 1,500 inpatient days per annum if using Aquilion ONE within the Emergency chest pain pathway instead of the traditional pathway. This represents 33% of the total annual capacity of AMU beds.

On average, per patient with acute chest pain approximately 519 could be saved with Aquilion ONE compared to the standard diagnostic pathway.

Projecting this to the annual patient population presenting with acute chest pain in A&E, i.e. for 4,000 patients in a typical hospital, annual savings of near EUR 1.8 million are possible.

The overall result was shown to be robust by the scenario analyses and it became clear that to achieve high cost and capacity savings it is crucial to use Aquilion ONE prior to sending the patients to AMU.

If the Aquilion ONE is used late in the pathway, there are still considerable, although smaller, savings.

The study concludes that further research is necessary to validate the new diagnostic pathway with Aquilion ONE and the cost calculation derived.

1 "Economic Value Modelling of the Use of Aquilion ONE in the Diagnosis of Patients with Acute Chest Pain Presenting to A&E"; Dr. Gerald Schnell Partner, and Tina Anne Schuetz, Consultant, Simon-Kucher & Partners.

Coronary Angiography and Myocardial Perfusion Imaging with 320-Detector Row CT Technology

T. Kühl, K. Fuglsang Kofoed

Multi-slice cardiac CT imaging has evolved as an important method for the clinical evaluation of coronary anatomy and prognosis in patients with suspec-ted or confirmed ischemic heart disease[1,2]. In recent years, CT technology has undergone a very rapid development resulting in decreased radiation dose, volume of contrast needed in addition to the time spent in the scanner for the individual patient. The introduction of the 320-detector row Aquilion ONE scanner has moved the important field of cardiac CT imaging into the next millennium, decreasing risk and optimizing patient comfort and image quality[3].

However, although decisive clinical information may be obtained in many patients using cardiac CT imaging, promoting a CT-guided treatment strategy, this is not always the case. It is not an uncommon finding that a coronary lesion may have intermediate stenosis severity[4] or that severe coronary calcification decreases the diagnostic accuracy of the test. In such cases additional testing is frequently needed, including radionuclide myocardial perfusion imaging with single photon emission computed tomography (SPECT) and magnetic resonance or echocardiography stress imaging, to determine the functional

Tobias Kühl, MD

Klaus Fuglsang Kofoed, MD, PhD, DmSc

Department of Cardiology and Radiology, Rigshospitalet, University of Copenhagen, Denmark

Case 1

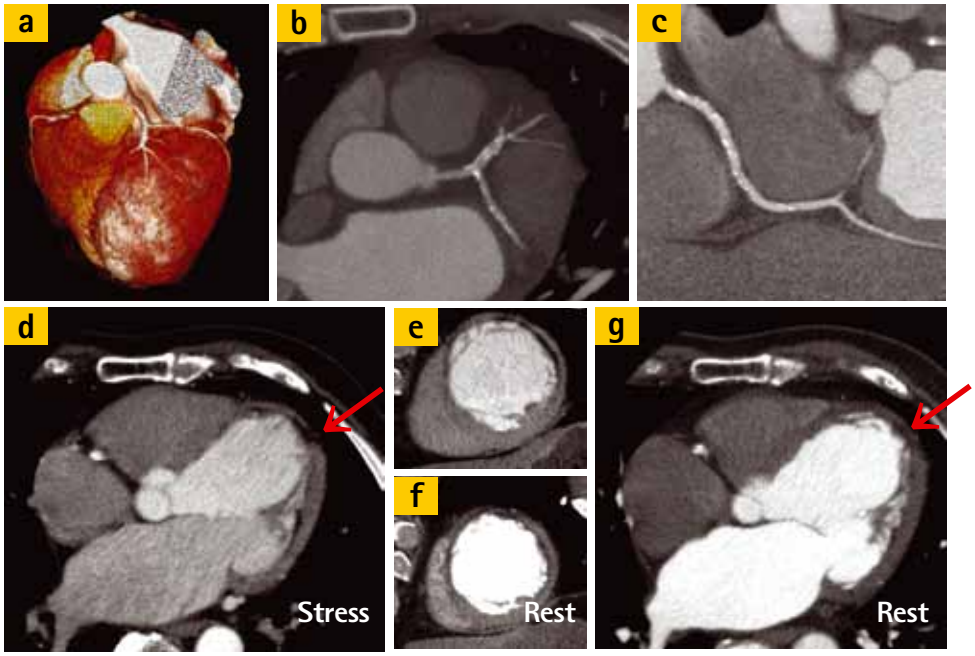

73-year-old male with known previous myocardial infarction and ischemic cardiomyopathy presented with new angina. The first part of the LAD and the D1 is severly calcified and it is difficult to determine from the CTA if there is a significant stenoses (b). The LAD is chronically occluded from its mid portion (a). The apical portion of the wall of the left ventricle is calcified. A large infarct is seen in the antero-lateral wall of the left ventricle (f,g). The myocardium is thinned. The stress images demonstrate the perfusion defect extending to the epicardial border of the myocardium (d,e). This indicates some reversible ischemia. The patient was referred for implantation of an ICD.

Case 2

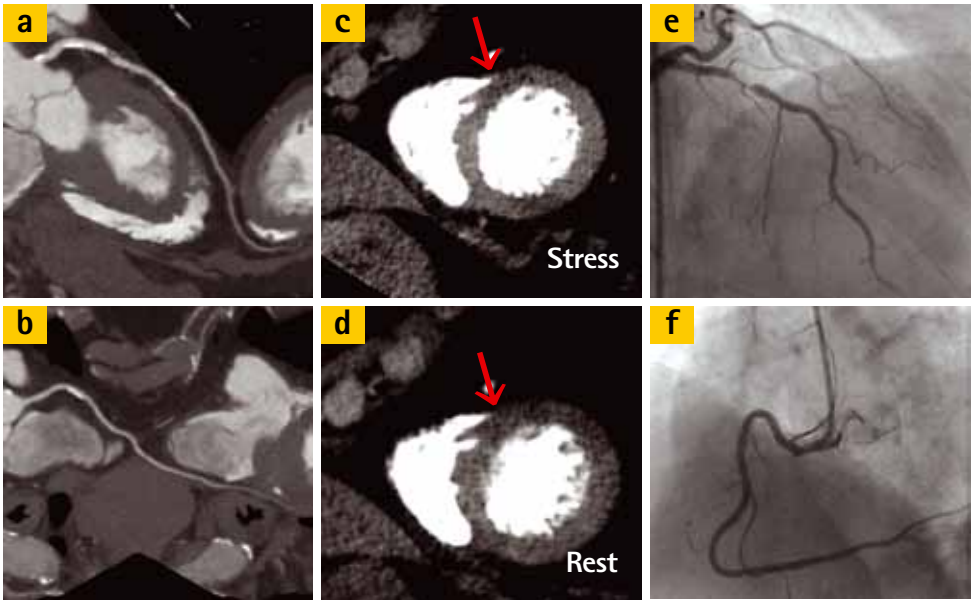

80-year-old female presented with unstable angina and shortness of breath. A calcified lesion is demonstrated in the proximal portion of the LAD (a). The degree of stenosis was considered to be >70%. Calcified and non-calcified lesions are also demonstrated in the proximal RCA (b). A low density area in the anterior wall is shown in the short axis stress and rest images (c,d). The location of the defect corresponds to the vascular territory supplied by the LAD and its branches. The defect is less pronounced on the rest images indicating partial reversibility and partial infarct. A stenosis of the proximal LAD was seen on the catheter angiogram (e). This lesion was considered to be causing an 80% stenosis. No lesion was apparent in the distal RCA (f). Based on the invasive angiogram results, the operator chose to perform stenting on the LAD lesion.

significance of such lesions in order to decide whether invasive coronary intervention should be performed.

Pioneering basic research efforts have been made to develop a coronary functional test using 320-detector row CT technology[5-7]. The 16 cm Z-axis coverage of the 320-detector row CT scanner allows for single-heart beat imaging and thus evaluation of instantaneous contrast distribution throughout coronary arteries[8] and the entire myocardium of the heart. Myocardial contrast distribution thus recorded reflects relative myocardial perfusion during diastole and may be measured at rest and during vasodilatation using intravenous adenosine. Accordingly, myocardial contrast distribution recorded at rest and during coronary vasodilatation permits evaluation of relative myocardial flow reserve. The heterogeneity of myocardial contrast distribution as a function of helical data sampling of multiple heart beats with older lower slice CT technology may be completely avoided. Combined anatomical and functional evaluation of coronary pathology using CT is a substantial step towards the development of the optimal non-invasive test for evaluation of patients with potential need for invasive revascularization. This has become possible by the introduction of myo-cardial perfusion imaging with 320-detector row cardiac CT. Here, we present two cases illustrating the clinical application of this new technique.

Conclusion

Combined CT coronary angiography and CT myocardial perfusion imaging is a very promising technique for a comprehensive evaluation of coronary pathology in patients with suspected or confirmed ischemic heart disease.

References

1 Abdulla J, Abildstrom SZ, Gotzsche O, Christensen E, Kober L, Torp-Pedersen C: 64-multislice detector computed tomography coronary angiography as potential alternative to conventional coronary angiography: a systematic review and meta-analysis. Eur Heart J 2007;28:3042-3050.
2 Abdulla J, Asferg C, Kofoed KF: Prognostic value of absence or presence of coronary artery disease determined by 64-slice computed tomography coronary angiography A systematic review and meta-analysis. Int J Cardiovasc Imaging 2010.
3 Dewey M, Zimmermann E, Deissenrieder F, Laule M, Dubel HP, Schlattmann P, et al.: Noninvasive coronary angiography by 320-row computed tomography with lower radiation exposure and maintained diagnostic accuracy: comparison of results with cardiac catheterization in a head-to-head pilot investigation. Circulation 2009;120:867-875.
4 Kristensen TS, Engstrom T, Kelbaek H, von der Recke P, Nielsen MB, Kofoed KF: Correlation between coronary computed tomographic angiography and fractional flow reserve. Int J Cardiol 2009.
5 George RT, Silva C, Cordeiro MA, DiPaula A, Thompson DR, McCarthy WF, et al.: Multidetector computed tomography myocardial perfusion imaging during adenosine stress. J Am Coll Cardiol 2006;48:153-160.
6 George RT, Jerosch-Herold M, Silva C, Kitagawa K, Bluemke DA, Lima JA, et al.: Quantification of myocardial perfusion using dynamic 64-detector computed tomography. Invest Radiol 2007;42:815-822.
7 George RT, Arbab-Zadeh A, Miller JM, Kitagawa K, Chang HJ, Bluemke DA, et al.: Adenosine stress 64- and 256-row detector computed tomography angiography and perfusion imaging: a pilot study evaluating the transmural extent of perfusion abnormalities to predict atherosclerosis causing myocardial ischemia. Circ Cardiovasc Imaging 2009;2:174-182.
8 Steigner M, Mitsouras D, Whitmore A, Otero H, Wang C, Buckley O, et al.: Iodinated contrast opacification gradients in normal coronary arteries imaged with prospectively ECG-gated single heart beat 320-detector row computedtomography. Circ Cardiovasc Imaging 2010;3(2):179-186.

First Experience with the 320-Row Detector in Otology

I.V. Bodrova, E.V. Fominykh, N.B. Gagarina, E.Z. Mukhamatullina

Initial reports on the usage of computed tomography in otorhinolaryngology were published in 1976 as data on ENT tomography. The temporal bone, the low resolution and long reconstruction time allowed evaluation only of the tympanum and external auditory canal wall. Modern CT systems, however, offer visualization of the Fallopian aqueduct, vestibule, window of the labyrinth and semicircular ducts as well as evaluation of auditory ossicles, both sequentially and separately. But imaging the finest structures of the temporal bone, for instance the stapedius muscle, is limited. The increase of spatial resolution and detector width to 16 cm on the Z-axis allows not only detection of hyperfine structures but evaluation of organ functions as well.

In February 2009, a CT system with a 320-row detector was installed in the Moscow Medical Academy named after IM Sechenov. Due to the increased detector width data on the static condition of temporal bone structures can be acquired with one rotation of the x-ray tube. Dynamic scanning allows functional visualization of auditory ossicles and their junctions and the ligamentous apparatus of the tympanum.

Irina V Bodrova, MD, PhD
Department of Radiology, State educational institution of higher professional education, IM Sechenov Moscow Medical Academy, Federal Agency of Healthcare and Social Development, Moscow, Russia

Fig.1: 3D reconstruction of labyrinth, front view. 1: upper semicircular duct, 2: horizontal semicircular duct, 3: posterior semicircular duct, 4: cochlea, 5: fenestra of vestibule, 6: fenestra of cochlea

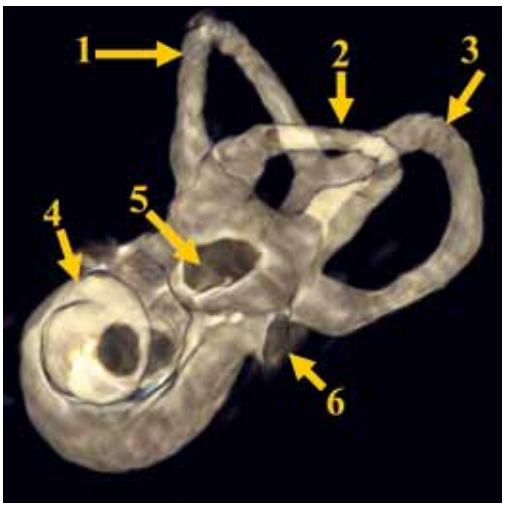

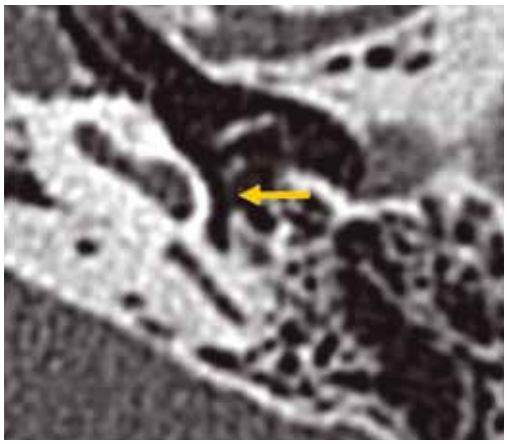

Fig. 2: Axial scan from patient R., 22 years old. Stapedius muscle is intact (arrow).*

These new possibilities demanded the development of efficient diagnostic algorithms for pathologies requiring functional evaluation. This article presents the first results of six months' work and of more than 50 examinations of patients with different ear diseases.

Static examination of temporal bones

We recommend this examination in predominantly inflammatory pathology. We use a volume scanning protocol at 120 kV, 200 mAs, with the patient being placed in a supine position. Tomography is performed in the area from the lower edge to the upper edge of the mastoid. Radiation exposure is 4.8 mSv. Postprocessing includes image reconstruction for each temporal bone with an increased field, 0.5 mm slice and 0.25 interval as well as multiplanar reconstructions. We recommend supplementing the processing of images with 3D reconstruction to allow a more precise visualization of spatial relations and of the labyrinth (Fig. 1).

This scanning protocol allows visualization of such fine structures of the temporal bone as the stapedius muscle (Fig. 2), base of stapes (Fig. 3) in 100% of cases.

* *Figures are presented in dynamic regime*

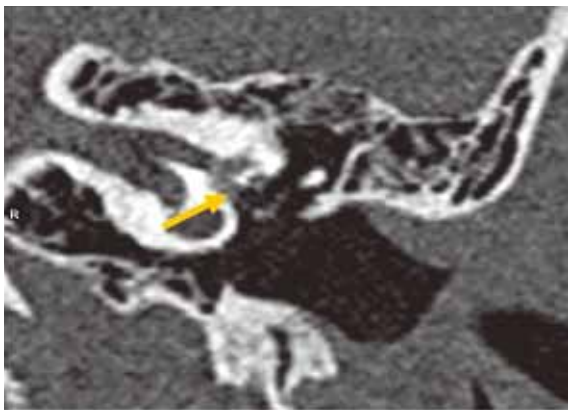

Fig. 3: Coronal scan from patient P., 27 years old. Fenestra of vestibule with base of stapes in it (arrow).*

High spatial resolution also allows the evaluation of the position of stapes prosthesie. Fig. 4 shows tomograms and 3D reconstructions from a patient after stapedoplasty. CT data is completely supported in revision of the tympanum.

The data obtained open possibilities for controlling the prostheses of auditory ossicles with CT, that is non-invasively which was impossible before systems with such resolution were developed.

Dynamic studies

Functional examination of auditory ossicles and of ligamentous apparatus of the tympanum is performed in the dynamic scanning mode. The wide detector allows continuous scanning of the temporal bone with a 16 cm coverage area with simultaneous air action on the tympanic membrane with a Politzer balloon with a 1 s interval (to provide movement of the chain of auditory ossicles). We use a scanning protocol with 80 kV, 300 mAs, scanning time 8 s which is sufficient for visualization of the whole range of movement. It must be noted that air action is performed on both sides in turn. Radiation exposure is 4.6 mSv for each temporal bone and 7 mSv for both. We consider that reconstruction with an increased field of view for each temporal bone is appropriate to improve spatial resolution. This method allows visualization of movements and their range for the malleus, incus and spates, with clear visualization of the action of malleo-incal and inco-stapeal junctions (Fig. 5), as well as of ligamentous apparatus of the tympanum (Fig. 6).

The study provides more precise diagnosis of adhesive otitis media and also can be useful for diagnosis of otosclerosis, because it allows the visualization of stapes and the stapedius muscle as well as membranes of vestibular and cochlear fenestra and evaluation of their range of movements.

After otitis and (or) trauma the tympanic membrane can be perforated or absent. Accordingly, inflation of air in the external acoustic meatus causes the risk of trauma of the chain of auditory ossicles. We propose to solve this problem by alternating dynamic study of auditory ossicles and ligamentous apparatus of the tympanum. Therefore, we also use a dynamic scanning mode with a 16 cm coverage area and with a simultaneous expiration maneuver for 1 s when nostrils and mouth are closed; the procedure is performed 4 times.

Scanning protocol parameters: 80 kV, 320 mAs, scanning time 8 s. Radiation exposure is 2.17 mSv. We strongly recommend performing postprocessing with image reconstruction with an increased field of view for each temporal bone. This method of

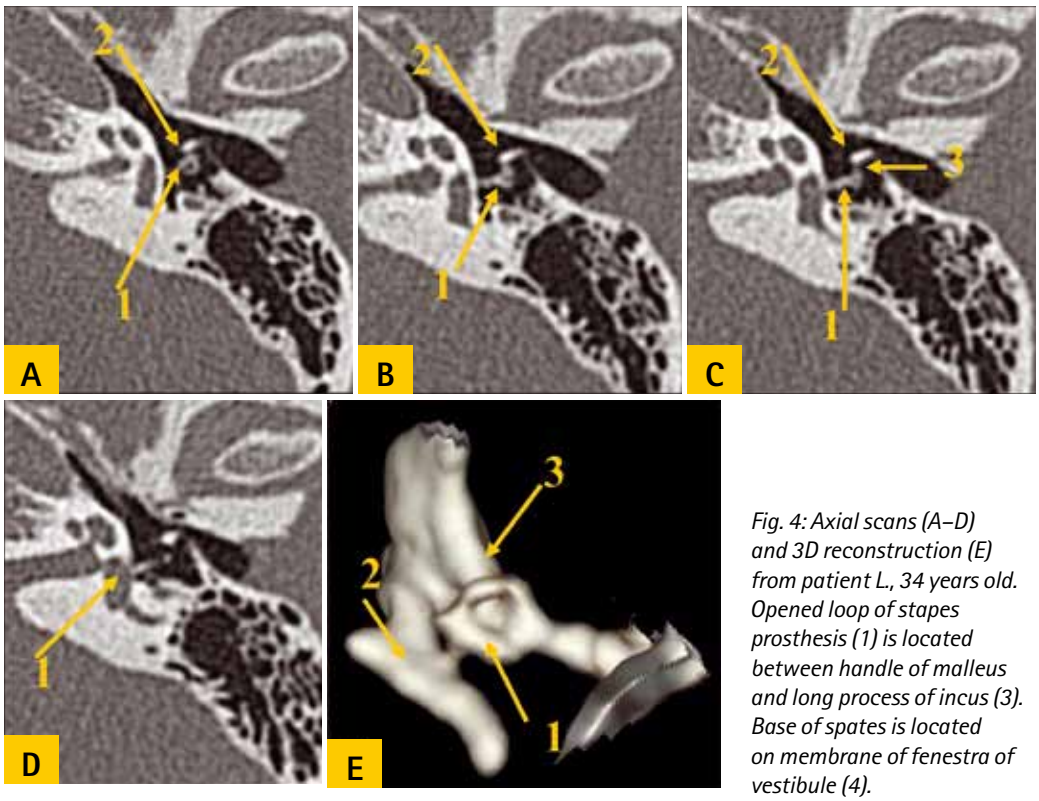

Fig. 4: Axial scans (A–D) and 3D reconstruction (E) from patient L., 34 years old. Opened loop of stapes prosthesis (1) is located between handle of malleus and long process of incus (3). Base of spates is located on membrane of fenestra of vestibule (4).

Fig. 5: 3D reconstruction of auditory ossicles. Interchangeable series of dynamic studies of auditory ossicles of patient B., 38 years old. Arrows show malleo-incal and inco-stapeal junctions.*

** Figures are presented in dynamic regime*

dynamic study cannot allow visualization of stapedius muscle movement in 100% of cases.

The Aquilion ONE system opens up possibilities of non-invasive examination of auditory tubes. Therefore, we also use a dynamic scanning mode with a 16 cm coverage area and with a simultaneous expiration maneuver for 1 s when nostrils and mouth are closed; the procedure is performed 3 times.

Scanning protocol parameters: 80 kV, 350 mAs, scanning time 6 s. Radiation exposure is 2.17 mSv. Tomography is performed in the area from the upper edge of the mandibular body to the upper edge of the mastoid. We consider that complete multiplanar reconstruction should be complemented with 3D reconstruction in a soft-tissue regime. The method of dynamic auditory tube CT that we developed allows the evaluation of the range of movements of the cartilaginous portion of the whole auditory tube (Fig. 7). Unlike contrast auditory tube CT, previously the only method of CT visualization of the organ, the proposed method does not require the performance of contrast injections and tympanic membrane perforation which greatly simplifies the study and is safer for the patient.

The unique features and characteristics of CT with a 320-row detector as well as the possibility of a volume dynamic scanner open fundamentally new possibilities of non-invasive visual diagnostics of ear diseases.

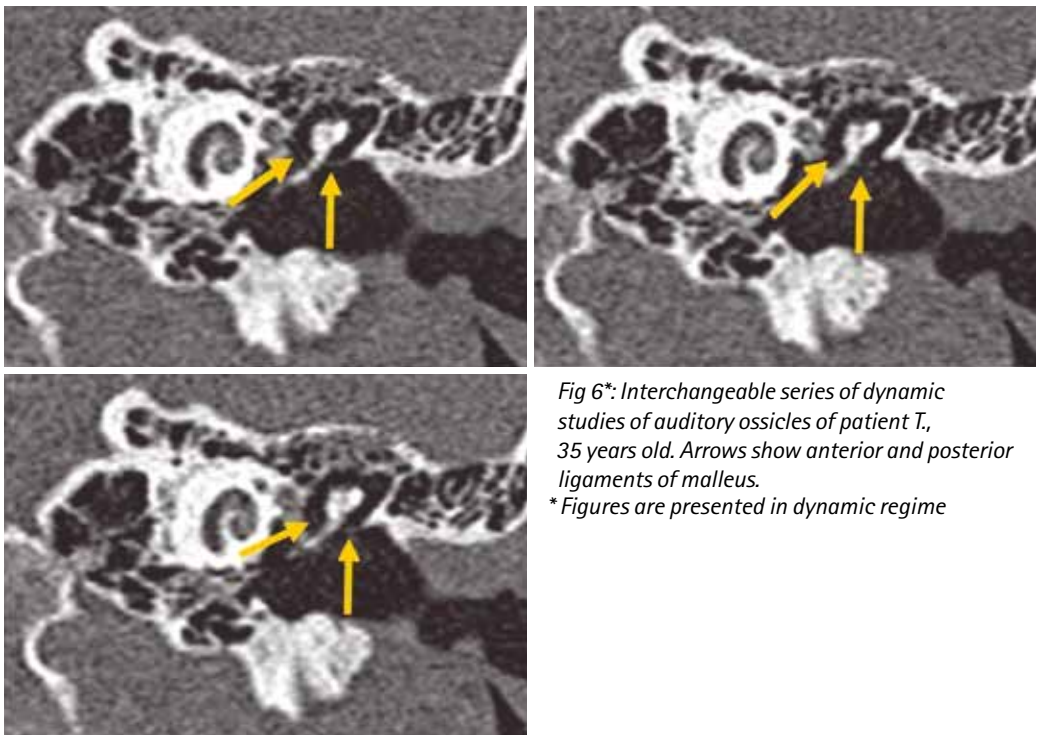

Fig 6: Interchangeable series of dynamic studies of auditory ossicles of patient T., 35 years old. Arrows show anterior and posterior ligaments of malleus.*
** Figures are presented in dynamic regime*

Fig. 7: 3D reconstruction of auditory tubes. Interchangeable series (A–D) of dynamic studies of auditory tubes of patient N., 28 years old. Arrows show opened and closed auditory tubes.*

** Figures are presented in dynamic regime*

Improved Image Quality in Clinical CT by AIDR

R.M.S. Joemai

Introduction

During the last ten years there has been a dramatic increase in the number of CT examinations performed worldwide. The introduction of multislice CT systems offering helical 3D scan techniques has allowed a wider range of diagnostic examinations. Reducing radiation dose has always been at the forefront of CT design. Technologies such as tube current modulation and active collimators are currently available in many CT scanners.

Recently, iterative reconstruction methods have gained popularity to generate clinical images with lower noise levels in comparison to the standard backprojection reconstruction method. The lower noise levels achieved by iterative reconstruction methods allow the radiation exposure to be decreased to noise levels and an image quality that are similar to the standard reconstruction method. Adaptive Iterative Dose Reduction (AIDR), available for the Toshiba Aquilion ONE/Premium/CX/64- and 32-slice scanners, is an example of this new technique. In this paper the image quality of AIDR is evaluated and compared to the standard reconstruction method.

Materials and methods

AIDR

When using an iterative process, the original high noise image undergoes a number of reconstructions that reduce image noise until the resulting image displays the desired noise level (Fig. 1). The final iterative image and the original image are weighted and combined to create the AIDR image. The weighted summation of the two images ensures that the edges of anatomy are preserved whilst the overall image noise is reduced.

Evaluation

To evaluate the image quality an anthropomorphic phantom was used (Fig. 2) and scanned on the Toshiba Aquilion ONE CT scanner.

The phantom consists of a skeleton and lung-tissue-equivalent material, surrounded by soft-tissue-equivalent material[1]. Two volume acquisitions were performed, one of the brain and one of the thorax. In the soft-tissue-equivalent material noise measurements were performed (methodology for noise measurements is described in reference 2). The results of the standard reconstruction were compared with the results of reconstructions with AIDR and displayed in graphs.

Two volume acquisitions were made by two rotations of 350 ms with an x-ray beam collimation of 320x0.5 mm. Tube voltage was 120 kV and the tube current varied in four steps 240, 120, 60 and 30 mA.

Also clinical studies were reviewed to visually compare standard and AIDR reconstructions. These studies include images of the brain and heart.

Volumes were reconstructed with and without AIDR at a slice thickness of 0.5 mm and a slice increment of 0.5 mm.

Raoul MS Joemai
Leiden University
Medical Center
The Netherlands

Fig. 1: Overview of the AIDR reconstruction process

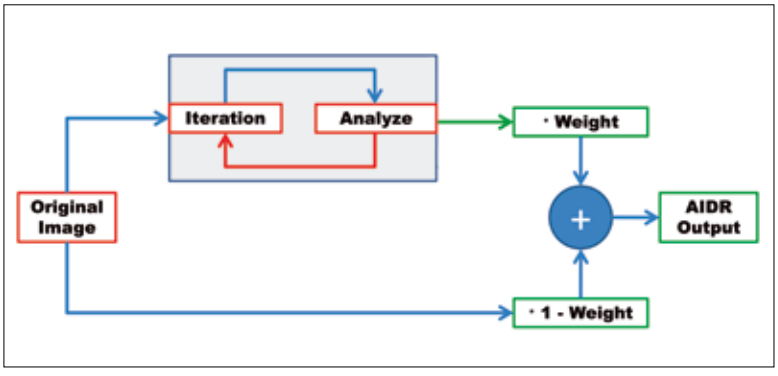

Fig. 2: Anthropomorphic phantom which contains a skeleton and lung-tissue-equivalent material, surrounded by soft-tissue-equivalent material.

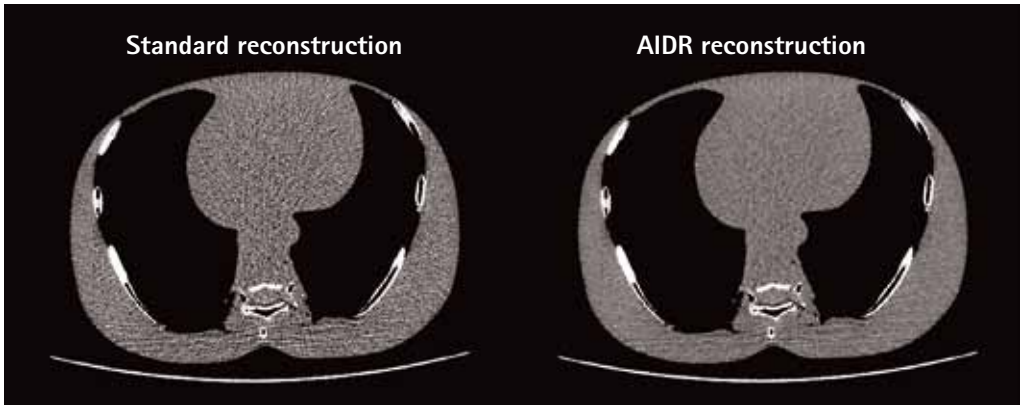

Fig. 3: Visual comparison of two reconstruction methods show a decrease of noise in AIDR reconstruction. Acquisition was performed at a tube current of 60 mA. Images are displayed with 400 window width, 40 window level.

Results

Visual comparisons of the anthropomorphic phantom between reconstruction methods show a reduction in noise within the entire scanned region (Fig. 3). Artifacts were not introduced or magnified.

Graphs in Fig. 4 show noise levels through the phantom. The coronal image in the background of the graph shows the relative position of noise measurements. AIDR reconstructions offered much lower noise levels in comparison to standard reconstructions at the same tube current level.

Noise levels for the standard reconstruction at 240 mA and AIDR reconstruction at 60 mA were very similar. Mean differences between standard and AIDR reconstruction for the brain reconstructions were 0.01±0.03% and for the thorax reconstruction -0.08±0.07%.

Results of applying AIDR to clinical studies are shown in Fig. 5. These include a study of the heart to visualize the coronary arteries and a study of the brain to visualize the blood vessels. In each study, AIDR results in significantly lower noise levels. Noise was also measured in a homogenous region of the heart, indicating a decrease in noise of 43%. To preserve an AIDR noise level similar to that of the standard reconstruction method, the dose saving can be calculated since the noise has an inverse square root relation with the dose. Dose saving in this example is 68% with AIDR. Noise measurements in the brain were not performed because of the inhomogeneous structure. Measurements in inhomogeneous parts with substantial anatomical noise can not be performed accurately. Results are visually compared and show again significant reduction in noise.

Conclusion

Reconstructions with AIDR showed no negative influences on image quality but a significant decrease of image noise. Thus radiation dose can be decreased in reconstructions with AIDR.

Fig. 4: Results of noise measurements in the anthropomorphic phantom at different tube currents. Two volume acquisitions were performed, of the brain and thorax. Left graphs (a) shows results of standard reconstruction right (b) shows AIDR reconstructions.

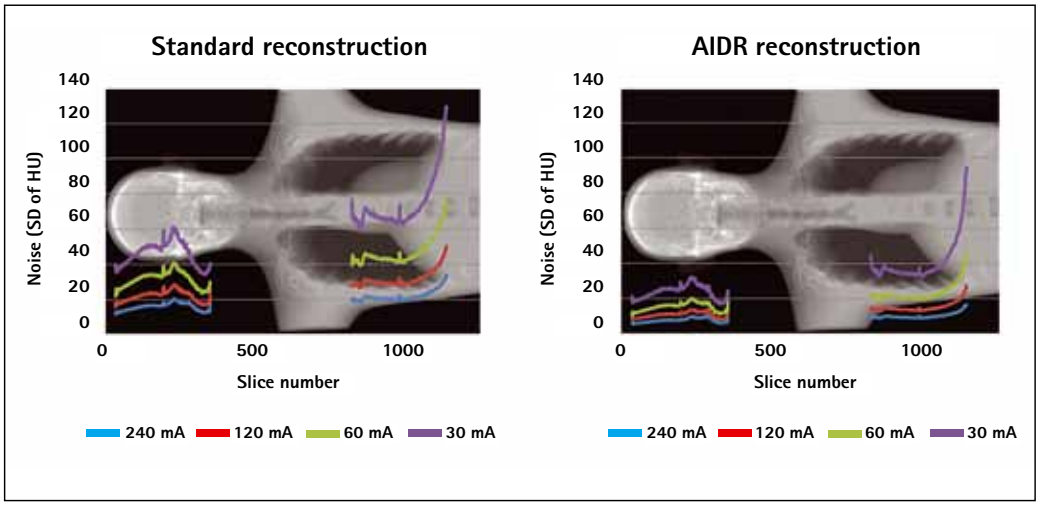

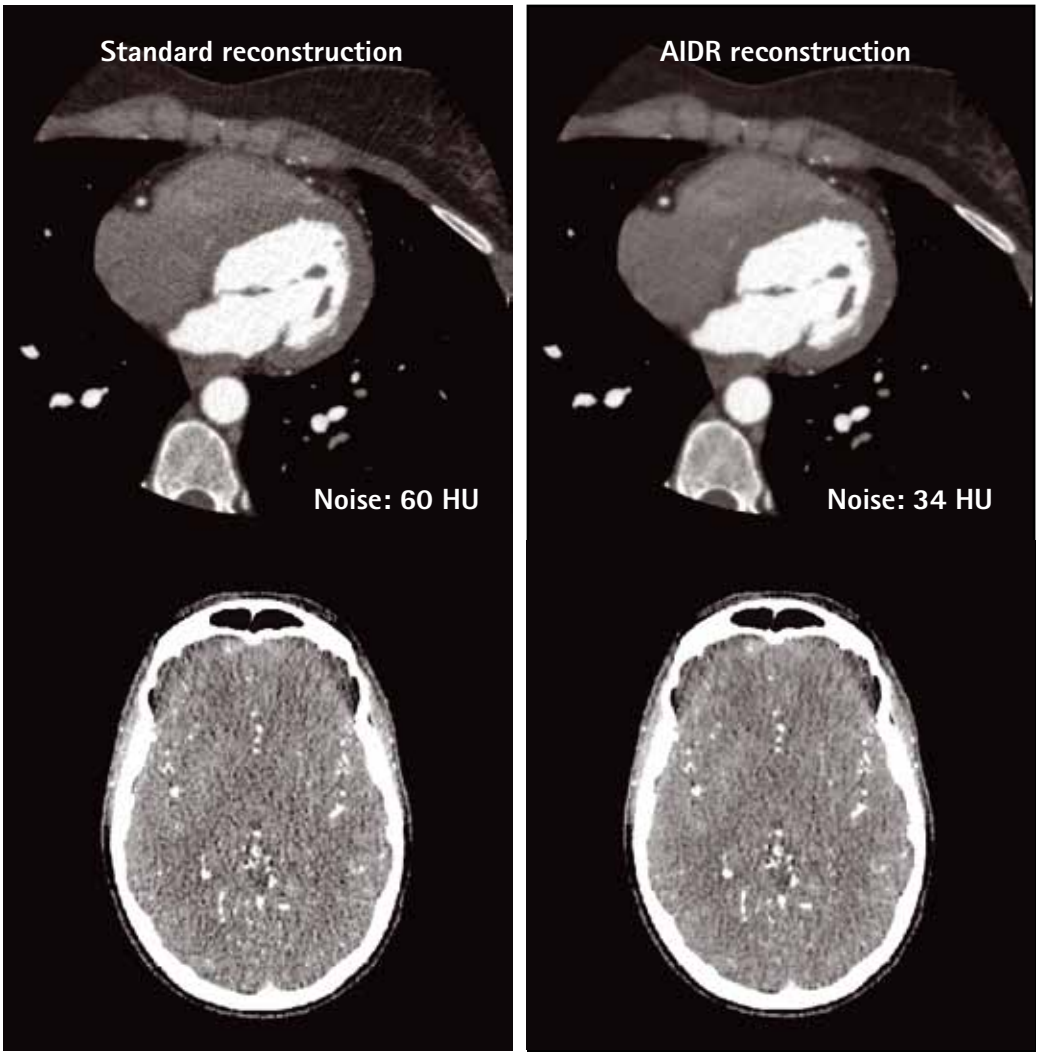

Fig. 5: Clinical examples of standard and AIDR reconstructions. AIDR reconstructions shows lower noise levels without loss of structures.

Iterative reconstruction methods were originally described in 1998 as a method to improve image quality by decreasing noise, improving low contrast resolution and reducing metal artifacts[3]. However, due to long reconstruction times iterative reconstruction was not used by any CT manufacturer. With improvements in computer processing speeds introduced to CT scanners, the processing times for iterative reconstruction methods have been reduced to a manageable level to enable them to be used in routine clinical workflows. Reconstruction time with AIDR is still longer compared to standard reconstructions but the differences are very small, i.e. 0.006 seconds longer per image for AIDR reconstructions.

In each analysis, lower noise levels were shown with AIDR reconstructions. The acquisition at 240 mA with standard reconstruction yielded noise levels comparable to those of the acquisition at fourfold lower dose (60 mA) with AIDR reconstruction. The effect of AIDR on clinical studies has shown to enhance the image quality. AIDR provides another opportunity to reduce radiation dose to the patient whilst acquiring diagnostic images of excellent image quality.

References
1 Shrimpton PC, Wall BF, Fisher ES. The tissue-equivalence of the Alderson Rando anthropomorphic phantom for x-rays of diagnostic qualities. Phys Med Biol. 1981 Jan; 26(1):133-9.
2 Joemai RM, Geleijns J, Veldkamp WJ. Development and validation of a low dose simulator for computed tomography. Eur Radiol. 2010 Apr; 20(4):958-66.
3 Wang G, Schweiger G, Vannier MW. An iterative algorithm for X-ray CT fluoroscopy. IEEE Trans Med Imaging. 1998 Oct; 17(5):853-6.

New 30x30 cm Detector with Compact Housing Enables Maximum System Utilisation

Fig. 1: Vascular surgeon Dr David Grosser (left) and cardiologist Dr Ross Sharpe (right) treat patients in the Toshiba Infinix VF-i Universal Interventional Angiography Suite with a 30x30 cm FPD at Allamanda Hospital

The hospital

Healthscope Allamanda Private Hospital is a 252-bed hospital located on Australia's Gold Coast. The hospital offers a wide range of services, from accident and emergency care to progressive surgical procedures, including orthopedic, neuro surgery, cardiothoracic surgery and vascular surgery. Given the hospital's broad patient mix, the interventional angiography suite must support a wide range of examinations.

The issue

Allamanda Private Hospital handles a mix of approximately 60% cardiology and 40% vascular/radiology cases which justified the purchase of an angiography suite. A versatile system was needed that could easily perform both types of studies in order to maximize utilization of the room while generating a steady cash flow to allow the hospital to recover the capital outlay required for the purchase.

The result

Toshiba's dedicated Cardiovascular Imaging Lab, which features a smaller 30x30 cm Flat Panel Detector (FPD) housing, was selected by Allamanda Hospital. This new FPD has external dimensions comparable to some dedicated cardiac 20x20 cm panels. It enables the steep angulations required for cardiac examinations to be set, while providing the benefits of a 30x30 cm field of view for vascular examinations.

The selection process

Flat panel detector (FPD) versatility

Staff members from the departments of cardiology, vascular surgery and radiology were involved in selecting a system that best met their combined needs. The hospital realized that a 30x30 cm FPD was a good size for nearly all radiological vascular examinations, and thanks to Toshiba's extra-small FPD housing, cardiologist were able to employ all the steep angulations required without compromise.

C-arm positioning to cover a range of examination needs

Toshiba's multi-access C-arm design was selected because it allows greater patient access than other systems during hybrid procedures such as ASD/VSD closures under transesophageal ultrasound guidance. In addition, examinations may involve anesthesiology staff and equipment that require free access to the patient's head. Lateral C-arm positioning allows good brachial access for cardiac imaging, and arm fistulograms can be obtained with optimal x-ray field collimation for easy radiological imaging.

Image quality

Toshiba's Advanced Image Processing (AIP) technologies with the Super Noise Reduction Filter permit fluoroscopy to be performed with no lag and also ensure that precise, clear images are obtained, even with steep angulations on large patients. Noise is also markedly reduced in DSA imaging.

Advanced technologies

Toshiba's Coronary 3D Stent Planner and Stent Optimizer are extremely helpful in both the planning and treatment assessment phases for the management of cardiac patients. 3D Angio Bone Fusion technology permits physicians and neurosurgeons to determine the best treatment option (surgery or catheter intervention) for patients with cerebral aneurysms. Bone Fusion not only displays bones and vessels in different colors but also allows the physician to show, hide or display in a semi-transparent mode either the bones or the vessels. This is extremely helpful to both surgeons and radiologists for procedure planning.

Fig. 2: Cardiologist Dr Michael Greenwood easily achieves 40° cranial angulations with Toshiba's rotating 30x30 cm FPD with a smaller housing.

Fig. 3: This 3D angiographic image of a selective carotid artery injection clearly depicts the cerebral aneurysm arising from the right A2 segment and involving the anterior communicating artery.

Dr Tom Snow
(Radiologist)

"I have performed a range of radiological examinations on the Infinix VF-i system at Allamanda Hospital, including endografts, discograms, vertebroplasties and even a paediatric barium swallow, utilizing prospective and retrospective fluoro store to reduce dose to the child. The system provides very nice imaging. The accurate 3D capabilities on the system add to the flexible case load we can offer to our referrers and patients."

Fig. 4: An endoluminal aortic stent graft was successfully placed below the renal artery extending to the femoral arteries, with an interesting twist. All of the relevant anatomy is easily included in the 30x30 cm field of view (FOV).

Dr John Bou-Samra
(Cardiologist)

"The lateral scissor movement of the 5-axis C-arm technology enables fingertip-to-fingertip imaging which is very useful for radial artery imaging. Also, the small FPD housing enables easy FPD movement into steep angulations, even on large patients."

Dr Ross Sharp
(Cardiologist and Vascular Interventionalist)

"If you look at the system in totality for me, as a cardiovascular interventionalist, it's a perfect fit. The 30x30 cm FPD allows me to get extreme C-arm angles with the plate close to the patient to minimise radiation exposure but then move to the leg and complete with 4 DSAs. We have about 10 cardiologists and 4 vascular interventionalists. I haven't heard a single complaint from either group regarding compromise. For me, being the only cardiac and endo-vascular interventionalist, I get to see how the system performs in both worlds and see great advantages."

Fig. 5: This fluoroscopic image was obtained with low-dose pulsed fluoroscopy, but the stents, markers, and balloon are all clearly visualized thanks to Toshiba's Advanced Image Processing (AIP) technology.

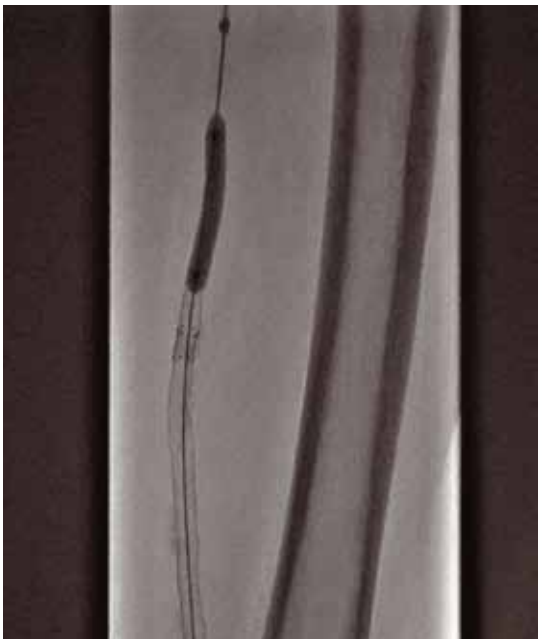

Dr David Grosser
(Vascular Surgeon)

"I like the 30x30 cm plate size from Toshiba because it offers excellent coverage of the areas of interest, but with the very thin housing, the FPD is further from my face. This lets me see my hands while manipulating wires and catheters whilst the FPD is in place, and improves radiation safety. Also, the maneuverability of the Toshiba C-arm permits me to work from either side of the table comfortably, for difficult-access examinations such as antegrade femoral punctures. Also the image quality is superb."

Fig. 6: A spider view with steep angulation clearly depicts the left coronary arterial system even when projected over the spine.

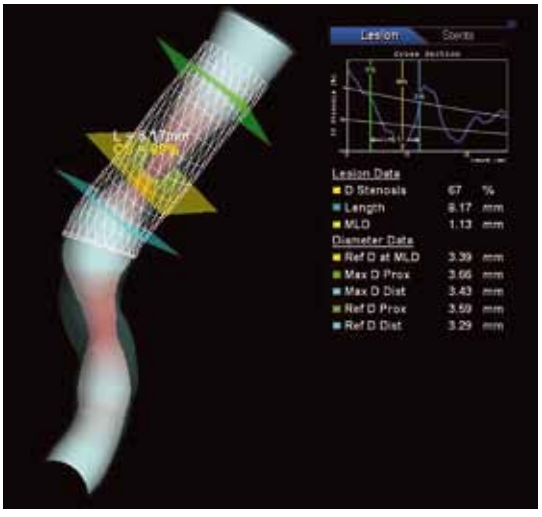

Dr Michael Greenwood
(Cardiologist)

"Initially I had reservations about the choice of a 30x30 cm plate, because my experience with 30x30 cm plates from other vendors influenced me to believe that angulation possibilities are limited. However, I have been pleasantly surprised by the Toshiba system. I often use steep cranial angles, and the Toshiba 30x30 cm plate with its small housing allows me to achieve these required angles as easily as on any smaller dedicated cardiac plate."

Fig. 7: Stent Planner with 3D QCA of the right coronary artery (RCA) was very helpful for selecting the correct stent and ensuring proper positioning in this interventional procedure.

From Standard Coronary Angiography to Double Rotational Angiography

Results of a retrospective monocentric register

M. Hanssen[1], O. Poitier[2], P. Couppié[1], F. De Poli[1], P. Leddet[1], P. Angot[2]

Introduction

Coronary CT scans have recently been used for morphological diagnostics of coronary arterial tree pathologies. Their advantage over standard coronary angiography (SCA) is the fact that they are non-invasive and that they can be performed on a strict outpatient basis. However, they are irradiating and require non-negligible doses of contrast medium. While their negative predictive value is excellent[1], their indications in the diagnostic decision tree are still limited[2].

Invasive coronary angiography is therefore still considered the gold standard. While it is currently a procedure with a low risk of complications, it still exposes patient, operator and medical team to radiation and of course it requires the use of contrast medium.

In order to advance SCA, a dynamic approach, based on rotation of the cradle during the selective injection of contrast medium, was introduced in 1998 in the evaluation of coronary disease[3]. Recently, the introduction of the flat panel detector, "mechanical" progress of catheterisation tables and progress in terms of IT allowed the development of rotational coronary angiography (RCA). This new procedure achieved two objectives: the reduction of radiation exposure and the reduction of the quantity of contrast medium.

The register presented here aimed at assessing these objectives with the help of a new system offered by Toshiba. In the first year of the system's operation, with technological innovations being progressively installed, we were able to compare SCA, "simple" RCA and double rotational coronary angiography (DRCA). Variations between operators were also studied.

Patient selection

For 250 patients, various parameters were recorded during and after each procedure, such as dose area product (DAP), fluoroscopy time, number of images produced, quantity of contrast medium used, body mass index, date of birth and the name of each operator as well as the associated radiological protocols. From January 2009 to May 2009, all patients were included in a non-selective manner and without exclusion criteria. Thus, the procedures sometimes encompassed ventriculography or additional explorations such as renal, abdominal, iliac or sigmoid angiography as well as bypass follow-ups.

All procedures beyond coronary angiography were subtracted retrospectively from the totals for DAP, fluoroscopy time and number of images. Only the quantity of contrast medium was not subtracted, since it was not registered for each sequence independently.

All data was entered in UNIMED, a software to manage anonymous patient records (UNIMED), and then extracted by a request module. This allowed preliminary analysis of this data.

Techniques

All procedures were performed on Toshiba's Infinix CFi, installed in April 2008 and comprising a single plane floor cradle, fluoroscopy pulsed in cardiological application of 10 images per second and two acquisition modes (10 and 15 images per second), a four-field flat panel detector (20x20, 17x17, 15x15, 11x11 cm), a "Live Zoom" electronic enlargement system, a double collimation system without the need to emit x-rays (semi-transparent mobile filters and lateral filters), an efficient 100 kW generator interfaced with an x-ray tube with three foci, one of which provides higher energy for scanning obese patients.

100 patients underwent SCA (static acquisition; 4 projections for the left coronary artery and 3 projections for the right coronary artery), 50 patients underwent RCA (right anterior oblique/left anterior oblique, then craniocaudal) and 100 patients underwent DRCA (right anterior oblique/left anterior oblique combined with craniocaudal).

These procedures were performed by four operators (3 experienced, 1 junior) and in all cases by femoral access.

The imaging techniques used varied according to the acquisition method.

In SCA, fluoroscopy was performed in a series of 10 images per second in a 1024^2 matrix with a low dose protocol, allowing a reduction of approx. 30%. In fluoroscopy and acquisition, the "Live Zoom" mode was used with a 1.2 factor, allowing the largest field (20 cm) to be maintained

Michel Hanssen
CH Haguenau
63 Bld René Leriche
67500 Haguenau, France

[1]Pole Neuro-Cardio-Vasculaire, CH Haguenau, 63 Bld René Leriche, 67500 Haguenau, France.
[2]Toshiba Medical Systems Europe B.V. Zilverstraat – 1 2718 RP Zoetermeer, The Netherlands

	DAP (Gy.cm²)		Fluoroscopy duration (min)		Number of frames (n)	
	Average	*Min-Max.*	*Average*	*Min-Max.*	*Average*	*Min-Max.*
SCA (n=100)	39.3	4.7-210.65	8.4	0.8-38	575	175-1427
RCA (n=50)	33.64	4.95-85.6	2.8	1.1-26	503	314-836
DRCA (n=100)	24.26	5.74-51.1	3.9	1.3-14	272	127-429

with the weakest combined dose, while having electronic image enlargement equivalent to a field of 17 cm. Additional copper-based filtration in the collimator was used (Ep = 0.3 mm).

Image acquisition was performed in a series of 10 images per second in a 1024² matrix.

In RCA, fluoroscopy was performed in a series of 10 images per second in a 1024² matrix with a low dose protocol, allowing a reduction of approx. 30%.

In DRCA, image acquisition was performed in a series of 15 images per second in a 1024² matrix, combined with a rotational speed of the cradle of 20 degrees per second in the combined axes.

Parameters studied

The parameters studied were preliminarily determined and prospectively recorded: 1) patient body mass index (BMI); 2) patient age; 3) quantity of contrast medium used; 4) fluoroscopy time in minutes; 5) number of radiographic images acquired; 6) DAP in Gy.cm², supplied by an ionisation chamber located at the exit of the x-ray tube. DAP, facilitating the routine measurement, is proportional to the equivalent dose (ED) received by the patient. The commonly used formula is: ED (in mSv) = 0.2 x DAP (in Gy.cm²).

Beginning with the start of the new service in April 2008, all parameters were recorded at the end of each procedure in UNIMED. Extraction of data, including the operators and the first and second actions, was carried out with the request application which is part of the software.

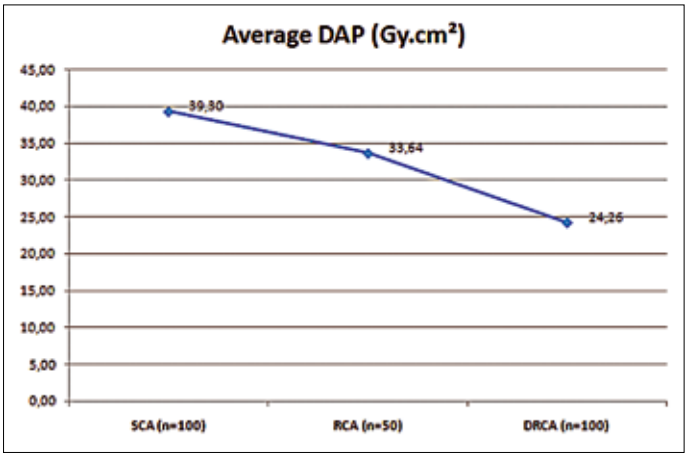

Fig. 1

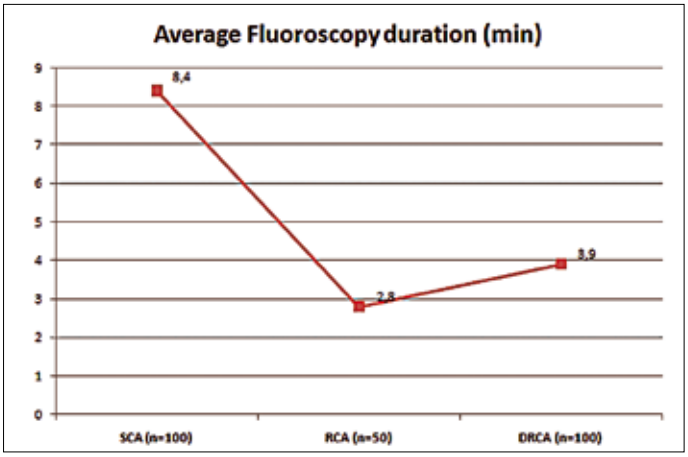

Fig. 2

Fig. 3

SCA	Examination	BMI (kg/m²)	No. Images	DAP (Gy.cm²)	Fluoroscopy time (min)
Operator 1	25	32.01	622	36.87	5.65
Operator 2	30	29.81	502	34.88	6.29
Operator 3	23	32.41	787	61.12	6.37
Operator 4	22	29.13	473	41.87	6.40

Table 2: Doses received by the patient in standard diagnostic coronary angiography per operator

DRCA	Examination	BMI (kg/m²)	No. images	DAP (Gy.cm²)	Fluoroscopy time (min)
Operator 1	24	30.52	282.00	23.90	3.26
Operator 2	34	30.44	279.00	21.49	4.61
Operator 3	21	29.17	287.00	25.87	4.59
Operator 4	21	31.78	313.00	25.87	4.82

Table 3: Doses received by the patient in double rotational diagnostic coronary angiography per operator

Results

The three populations studied were:

- 100 patients in SCA: average age 67 years [37-89], 69% men, average BMI 28.5 kg/m² [16-40] with 29% presenting with obesity defined by a BMI ≥ 30 kg/m².
- 50 patients in RCA: average age 64 years [28-81], 58% men, average BMI 27 kg/m² [18-36], of which 40% ≥ 30 kg/m².
- 100 patients in DRCA: average age 64 years [34-85], 59% men, average BMI 29 kg/m² [17-41] of which 33% ≥ 30 kg/m².

The exposure data (DAP, radioscopy time and number of images) for all examinations with the three techniques performed between January 2009 and May 2009 are shown in Table 1 and Figures[1-3].

Compared to SCA, RCA showed a significant reduction of DAP (-14%), accompaned by a reduction of fluoroscopy time (-67%), number of images acquired (-13%) and quantity of contrast medium (-38%).

DRCA showed an even more significant reduction of DAP (-38%), number of images acquired (-53%) and fluoroscopy time (-54%). The reduction of quantity of contrast medium, however, was less pronounced (-29%).

It has since been determined that this less significant reduction is due to the fact that DRCA requires a finer adjustment to the isocentre than RCA. Consequently, fluoroscopy time is higher in DRCA than in RCA (+3%).

The quantities of contrast medium are not, at first glance, exploitable. Nevertheless, the retrospective analysis of a patient who only underwent SCA without any secondary procedure showed that 41% of the patients who underwent a coronary angiography in DRCA received an average quantity of contrast medium of 53 ml [24-110].

A second analysis was carried out regarding radiation exposure of patients by operator. Here, only SCA and DRCA were compared.

Exposure data (DAP, fluoroscopy time and number of images) for all examinations with the two techniques are shown in Tables 2 and 3.

The number of procedures and the patient data were homogeneous for the four operators (1-3: senior operators; 4: junior operator.

The results of the exposure data (DAP, fluoroscopy time and number of images) for all examinations with the two techniques are shown in Table 4.

Overall, DAP by all four operators is clearly reduced. The average values show a reduction in the number of images acquired (-54.7%) for operator no. 1 (experienced), accompanied by a reduction of DAP (-35.2%) and of fluoroscopy time (-42.3%). Operator no. 2 (experienced) records a lesser reduction of the number of images (-44.4%), of DAP (-38.4%) and also of fluoroscopy time (-26.7%). This lesser reduction can be explained by the fact that this operator had already achieved minimum values for SCA, and therefore the decrease is in absolute values lower than for the other operators. Operator no. 3 (experienced) significantly reduced the number of images acquired (-63.5%) as well as DAP (-57.7%) and fluoroscopy time (-27.9%). Operator no. 4 (junior) also reduced the number of images acquired (-33.8%), DAP (-38.2%) and fluoroscopy time (-24.7%).

The data collected shows a reduction in the quantity of contrast medium in DRCA. For operator no. 4, however, this value has markedly increased (+3.6%) without us having been able to determine the cause.

Discussion

The results of the comparison of SCA and DRCA show a very clear reduction of fluoroscopy time (-54%) and in a same proportion of the number of images acquired (-53%). We expected DAP to be reduced in the same proportion, but in fact this reduction was less significant (-38%). This is primarily due to the fact that the source-detector distance is markedly increased in order to allow homogene-

Case 1

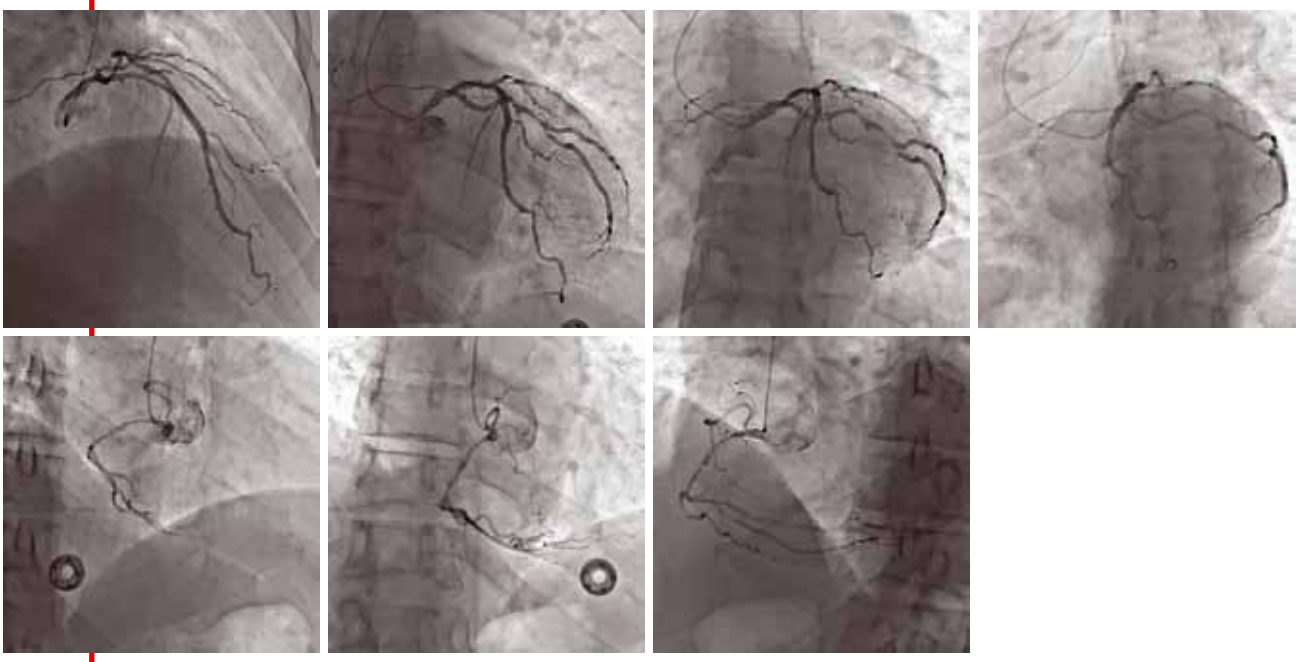

ous rotation around the patient to the isocentre and with no risk of collision or withdrawal. In coronary angiography, it is acquisition time rather than fluoroscopy time that impacts DAP. It is useful to remember that the dose per image is eight to ten times higher in acquisition mode than in fluoroscopy mode. Consequently, we can assume that a reduction of DAP is accompanied, on average, by a similar reduction factor only in acquisition for similar protocols. This is well observed for RCA where, compared to SCA, the reduction of the number of images acquired (-14%) is directly linked to a reduction of DAP (-13%) whereas fluoroscopy time is reduced drastically (-67%).

It is well determined that in SCA the total radiation dose is linked to certain factors such as radiation time (fluoroscopy and fluorography), series of images, type of incidences, field size, use of the collimation and use of an additional filter. The introduction of flat panel detectors, in relation to the classic image intensifier, should certainly not mean that these inescapable principles of radioprotection

Table 4: Comparison of the doses received by the patient per operator

	SCA versus DRCA			
	No. images	*DAP (Gy.cm²)*	*Fluoroscopy time (min)*	*Contrast (ml)*
Operator 1	-340 **-54.7%**	-12.97 **-35.2%**	-2.39 **-42.3%**	-41 **-31.3%**
Operator 2	-223 **-44.4%**	-13.39 **-38.4%**	-1.68 **-26.7%**	-21 **-22.3%**
Operator 3	-500 **-63.5%**	-35 **-57.7%**	-1.78 **-27.9%**	-18 **-12.7%**
Operator 4	-160 **-33.8%**	-16 **-38.2%**	-1.58 **-24.7%**	4 **3.6%**

Case 2


LCA Rao44/Cau28


LCA Rao29/Cau14

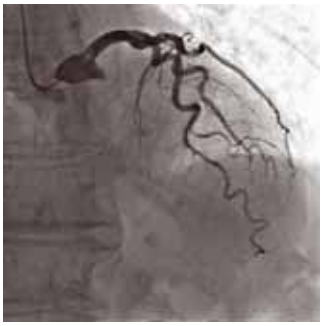
LCA Rao06/Cra10


LCA Lao10/Cra25


LCA Lao26/Cra30


LCA Lao30/Cra30


RCA Lao88/Cra0


RCA Lao48/Cra0


RCA Rao01/Cra0


RCA Rao29/Cra0

are forgotten. As regards the radiation exposure of the staff performing the procedure, these principles are of course still valid. They must be combined, in terms of radioprotection, with classic systems, if possible the new injection systems (ACIST or MEDRAD) which allow the operator to be further away from the x-ray tube.

In line with previously reported results we observed on average a significant reduction of DAP in RCA compared to SCA and in DRCA compared to RCA. Furthermore, the level of contrast medium used in DRCA compared to SCA is also significantly reduced.

If we look at the results per operator, operator no. 3 (senior) uses significantly more radiation in SCA than the three others. As the technical characteristics of the procedure are strictly superimposable, this is only linked to the number of procedures preferred by this operator for their diagnostic interpretation. In DRCA, we see a homogenisation of DAP between the various operators, but this result is a little "artificial" given the homogeneous predetermination of the two double rotational procedures on the left coronary artery and the double rotational incidence on the right coronary artery for all operators.

In the PDS GACI 2006 survey on dosimetry in interventional cardiology carried out by Bar and Maccia, the average DAP in SCA is 56 Gy.cm² (5-291 Gy.cm²). The diagnostic reference level in Europe is 57 Gy.cm². In our centre, average DAP, whether in SCA, RCA or DRCA, is much lower than this reference value and the average value of the GACI survey. This difference will be more significant when comparing SCA to DRCA (cf. Table 1). Our centre participated in the GACI 2006 survey. At that time, the same operators worked in a room with an image intensifier. In 2006, average DAP of the same operators was 54.6 Gy.cm² in SCA. We thus ob-

serve a significant reduction of average DAP in SCA between the catheterisation room used in 2006 and the one used for this register (54.6 Gy.cm² versus 39.3 Gy.cm²). Regardless of the dynamic possibilities of rotational coronary angiography, this very clear reduction is linked to the technological possibilities that are currently available and to their optimised use. It is important to remember that for every new catheterisation room and regardless of the staff involved, the initial regulations are "factory-set" and need to be adapted on site according to the normal working customs, imaging preferences of the operators, type of patients, etc.

All procedures were performed via femoral access. Certain authors[4] report higher radiation for radial access.

Our register has significant limitations: there was no randomisation; RCA and DRCA results were "refined" from the data of the additional procedures, possibly preferred by the operator; there was no protocol for patient selection. It therefore is more of an observational study, reflecting the real-life situation and the progressive deployment of the technology of a new catheterisation room in its first few months of operation.

However, the literature corroborates the results described here. A randomised trial[5] of SCA versus RCA shows a reduction of contrast medium by 33% (52.8 versus 35.6 ml) and of DAP by 28% (53.9 versus 39 Gy.cm²). Another randomised trial of the same type[6] finds a DAP reduction of 36% and of total dose of contrast medium of 33% in favour of RCA. A third randomised trial[7] shows a reduction of 40% for contrast medium but no difference in terms of DAP. This is explained by the authors as being linked to a drastic optimisation of SCA prior to the use of RCA.

Another limitation of our register is the absence of a quantifiable comparison of the lesions between SCA and DRCA, but such a comparison would have required SCA and DRCA to be performed for each patient. This was done in a trial[8] and shows high reliability ith regard to the detection and quantification of coronary lesions. Moreover, the same results were recorded in a previously cited[6] trial.

Conclusion

The clarified use of the technological possibilities of modern catheterisation rooms allows a significant reduction of patient radiation exposure in SCA. This reduction and the added reduction of contrast medium are even more pronounced in DRCA, if used exclusively. It remains to be determined which patients can benefit from DRCA as a replacement and/or supplement of SCA. Dynamic rotational coronary angiography is evidently a new advanced technology but contrary to the peripheral vascular diagnostic evaluation the time of real three-dimensional coronary angiography has not yet arrived.

References
1 Sirol M, Sanz J, Henry P, Rymer R, Leber A. Evaluation of 64-slice MDCT in the real world of cardiology: A comparison with conventional coronary angiography. Archives of Cardiovascular Disease (2009) 102, 433-439.
2 Christiaens L. Coroscanner: quelles indications dans les cardiopathies ischémiques. AMC pratique, no. 178, May 2009.
3 Tommasini G, Camerini A, Gatti A, Derchi G, Bruzzonz A, Vechio C. Panoramic coronary angiography. J Am Coll Cardiol 1998; 31:871-7.
4 Blanpain T, Duval S, Tourneux C, Deschildre A, Brasselet C. Principes de radioprotection en cardiologie interventionnelle. CAT'LAB, June 2009.
5 Maddux JT, Wink O, Messenger JC, Groves BM, Lia R, Strzelczyk J et al. Randomized study of the safety and clinical utility of rotational angiography versus standard angiography in the diagnostics of coronary artery disease. Catheter Cardiovasc Interv 2004;62:167-174.
6 Smida W, Sidéris G, Stratiev V, Logeart D, Ouadhour A, Tarragano F et al. Angiographie coronaire rotationnelle. Arch Mal Cœur Vaiss, Nov. 2007, volume 100, no. 11.
7 Akhtar M, Vkahria KT, Mishell J, Gera A, Ports TA, Yeghiazarians Y et al. Randomized study of the safety and clinical utility of rotational vs. standard coronary angiography using a Flat-Panel detector. Catheter Cardiovasc Interv 66:43-49 (2005).
8 Garcia JA, Agostoni P, Green NE, Maddux JT, Chen SY, Messenger JC et al. Rotational vs. standard coronary angiography: An image content analysis. Catheter Cardiovasc Interv 2008 Dec 9.

The New CV-3D plus Stent Planner, Stent Optimizer and Stent Fusion

Innovative technologies assist cardiac interventional doctors in a variety of clinical scenarios

Introduction

Toshiba's CardioVascular 3D system CV-3D™ is continually providing new features for the interventional cardiac market. The newest additions to the CV-3D are advancing clinical applications to 3D lesion assessment and measurement. These features are useful in procedure planning for difficult, complex, tortuous and bifurcated lesions. Interventional device placement and post-stent deployment assessment are key features of the cardiovascular suite. Stent Fusion allows assessment of stent wall versus vessel wall for improved stent deployment

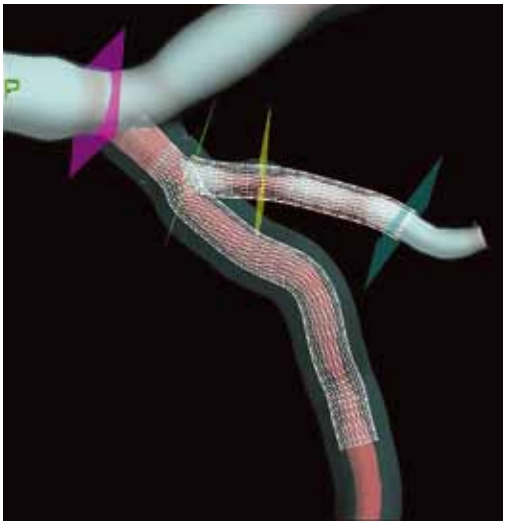

assessment. Biplane synchronous replay is also available to assess 2D images in two planes on one screen.

Assessment of lesions with CV-3D

CV-3D versus 2D QCA

2D QCA measurements have some inaccuracy in certain angles due to the foreshortening of vessels. The graph to the right shows the length measurements by 2D QCA and by CV-3D of a 13.96 mm phantom vessel projected at 5° increments. The 3D QCA measurement is 13.58 mm while 2D QCA shows a length of 9.87 mm for the true length of 13.96 mm.

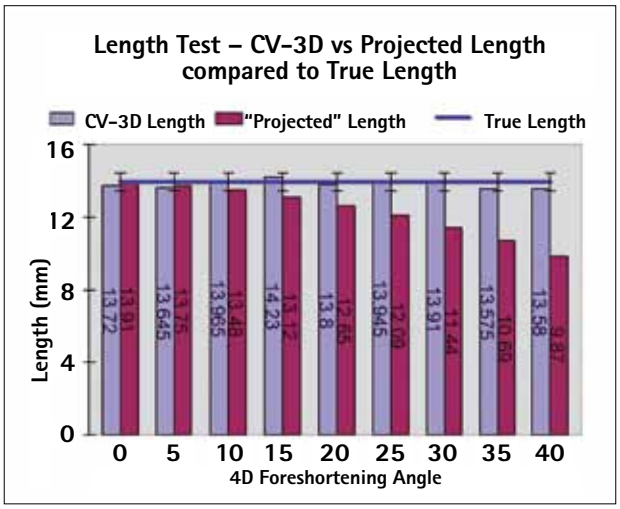

This proves that 3D QCA offers increased accuracy across the full range of projections compared to 2D QCA.

CV-3D versus IVUS

It has been reported that "three-dimensional angiographic measurements of intermediate coronary lesions (50-70%) correlate well with measurements using intravascular ultrasound," as Bermudez, Collingwood and Fischell from Borgess Medical Centre, Kalamazoo, Michigan, USA, stated in their poster presentation at ACC in Chicago, 2008.

The study involved 31 patients and 32 lesions using both IVUS and CV-3D. This measurement accuracy combined with the ease of use and speed of the CV-3D system in many situations may lead to 3D QCA being used as a low cost, less invasive alternative to IVUS when accurate lesion length measurement and not plaque morphology is the reason for investigation. This speed is extremely important for hospitals where reducing door-to-balloon (D2B) times of STEMI patients is a focus.

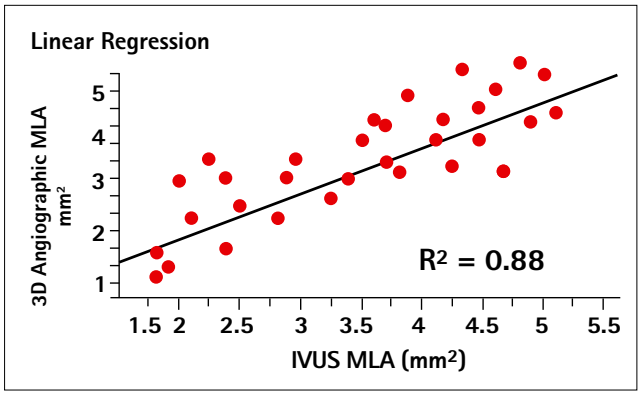

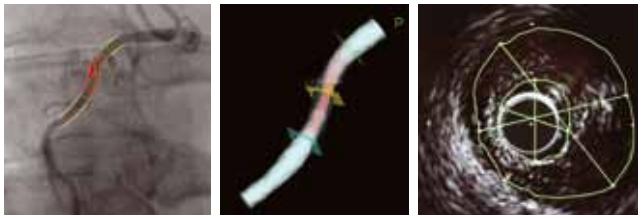

Add stent window of CV-3D software

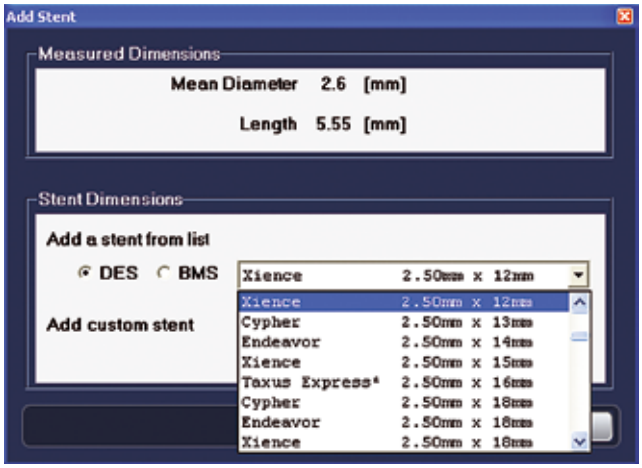

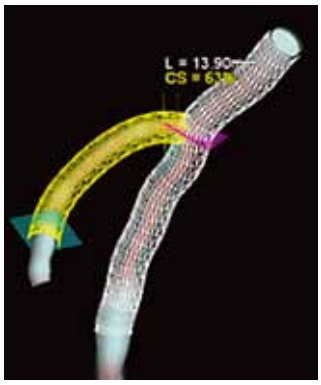

Bifurcation stents bifurcation vessel not in profile

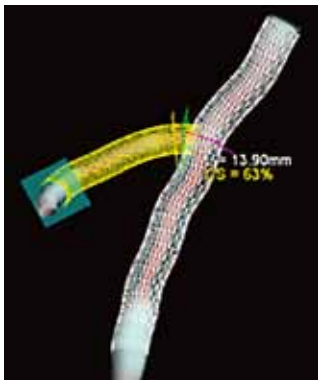

Bifurcation stents in profile after rotation

Planning the procedure

Stent Planner – a unique advantage

The CV-3D offers a unique function, Stent Planner, which shows a virtual stent over the 3D coronary arteries of the 3D QCA image. A virtual stent can be selected from a customizable list of stents, visualized over the artery and moved along the artery into the exact position. Stent Planner technology can help the doctor to judge more accurately the correct stent length and to plan the correct size of the stents as well as their correct positioning in relation to branching arteries.

Also, multiple stents can be planned on one patient, which means that Stent Planner is well suited to prepare more difficult examinations involving tortuous vessels, long lesions requiring multiple stents and difficult bifurcation lesions. By seeing the stent overlap in the bifurcation image, the doctor can determine where to place the bifurcation branch stent so that the risk of blocking-off the main branch is reduced.

The 3D multi-branch display can be rotated so that bifurcating arteries are in profile, and branch stents can be accurately positioned relative to main vessel stents as in the example shown in the images to the right. Stent Planner can be used as a tool to help cardiologists who are learning intervention to accurately select their stents and to visualize the positioning of stents in relation to other stents or branches before stent selection, positioning and deployment. This more accurate stent selection and positioning planning can lead to positive patient outcome and more efficient use of catheter laboratory budgets.

In which clinical situations can Stent Optimizer be helpful?

Stent Optimizer's best known application is determining stent apposition against the artery wall after stent deployment. While this is still the primary use of the Stent Optimizer technology, other useful clinical applications are becoming apparent with the use of this technology.

Stent apposition analysis after stent deployment

After deployment of a stent, Stent Optimizer can show that the stent is underexpanded and requires post-deployment balloon inflation. The CV-3D software can display an outline of the stent and a graph showing the percentage of underexpansion compared to the rest of the stent. By better visualizing the stent apposition against the wall of the artery and correcting the underexpansion of the stent, the risks of stent thrombosis and re-stenosis are minimized.

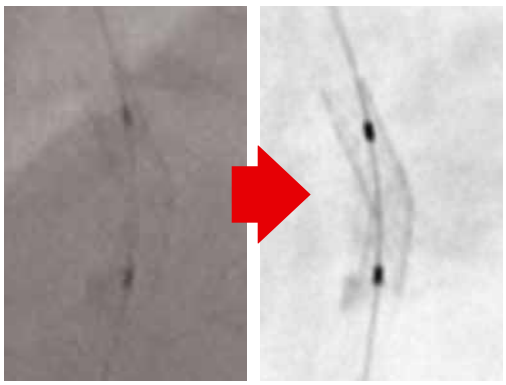

Digital aquisition *Stent optimized*

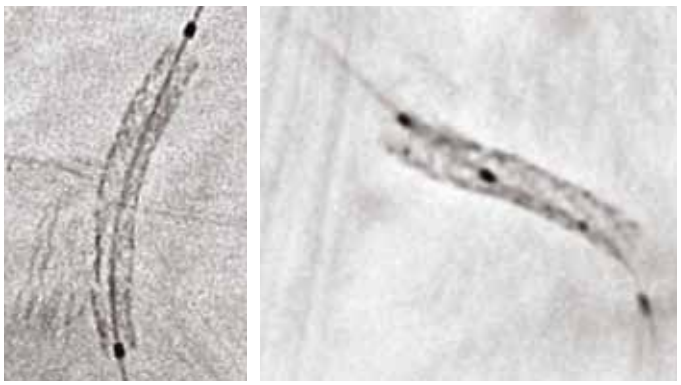

Chest wire subtracted Stent Optimizer image *Catheter subtracted Stent Optimizer image*

1st optimized balloon position *The balloon is then moved to a better position* *Optimized image shows balloon in position*

Balloon positioning without contrast media
After Stent Optimizer has determined an underexpanded stent, balloons placed inside that stent for post-deployment inflation can easily be positioned without the use of contrast media which is particularly helpful for patients with poor renal function.

Optimized image displaying clear stent overlap

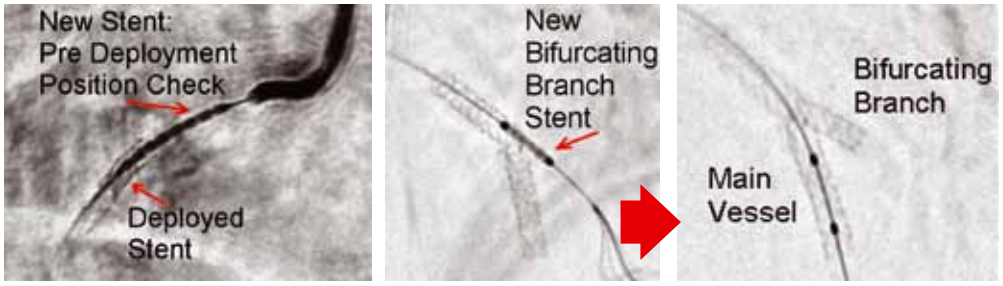

Optimized assessment of branch stent position *Stent Optimizer result: bifurcation stenting*

Additional stent positioning without contrast media
Placing stents with optimal overlap can reduce the potential for re-stenosis. Stent Optimizer can be used to position the new stent inside the deployed stent, allowing accurate visualization of stent overlap prior to second stent deployment. The new stent can be repositioned and enhanced multiple times to see the stents relative positioning and overlap without the need to use additional contrast media for new position confirmation. Stent Optimizer can be useful in bifurcation lesion stenting to determine the branch stent's relationship to main vessel stents.

Subtraction of chest wires or catheters

Stent Optimizer has been shown to subtract chest wires from the enhanced image on patients who may have had coronary artery grafts. This phenomenon can be very helpful when the chest wires would have otherwise obstructed the view of the stent. The entire stent can now be analyzed. Stent Optimizer has also been shown to subtract catheters which are close to the enhanced stent.

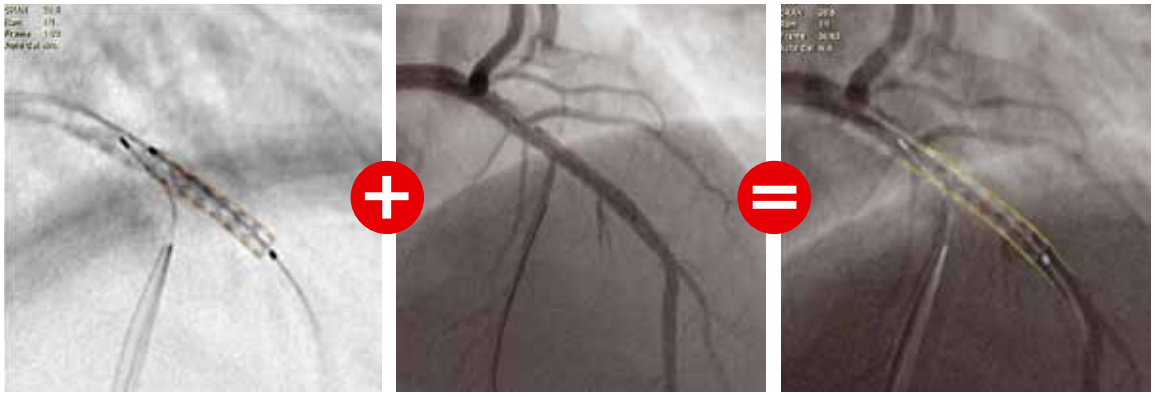

Enhanced stent *Vessel* *Stent Fusion*

Stent Fusion
Stent Fusion allows doctors to visualize an enhanced stent fused with a contrast filled artery angiographic image. A stent borderline and artery borderline can be displayed to easily demonstrate the areas of mismatch between the wall of the artery and the stent. The display can also be changed to show more stent or more artery.

Tableside integration of Stent Optimizer

The combined features and latest technology of the CV-3D on the Toshiba InfinixTM-i series angiographic system can enhance images very easily using the tableside control. The results of each enhancement can be seen in real-time in the examination room using the extra monitor display option.

Synchronized biplane replay

The CV-3D has a synchronized biplane replay function which can play runs taken at different angles at the same time. This is extremely useful for left ventricular analysis from RAO and LAO planes to be viewed at the same time in synchronous movement.

CV-3D supports interventions at many stages of the procedure

CV-3D functions help physicians at different stages of the cardiac interventional examination. Integration of certain features into the tableside control make workflows faster and operation easier. Visualization of the CV-3D images on Toshiba's extra monitor display option allows real time display of results in the examination room. The CV-3D requires no special additional runs to create a 3D image of the coronaries. Stent Planner allows visual confirmation of multiple virtual stents from the customizable stent database to be positioned over difficult lesions, including main vessels and branch arteries. Stent Optimizer can be used to assess deployed stent apposition against the vessel wall. Stent Fusion technology allows visual confirmation of the Optimized Stent displayed in a fusion overlay with the artery. Tableside control to enhance stents using Stent Optimizer allows fast, easy operation with minimal and in some cases zero contrast media usage during balloon positioning for post-deployment inflation and stent positioning in multi-stent cases where patients run a high risk of renal complications due to large volumes of contrast media usage. Therefore, CV-3D features provide doctors with excellent tools for planning, measuring, improved visualization, assessment and position planning related to other stents or branches and even in repositioning of therapeutic devices during interventional examinations on Toshiba's Infinix-i series interventional angiographic systems.

The New Lighting Innovation

To achieve the same performance as a standard light bulb, E-CORE™ will use 80% less energy, will last 40 000 hours and will be resistant to shocks and vibrations, something of a revolution for the traditional light bulb.

A Toshiba LED light bulb produces practically no ultraviolet or infra-red emissions and contains no mercury.

Take control of your energy consumption and your spending whilst reducing your lighting system's carbon footprint with E-CORE™ by Toshiba.

Toshiba also offers a complete range of high-performance lighting products.

TOSHIBA
Leading Innovation

TOSHIBA
Leading Innovation

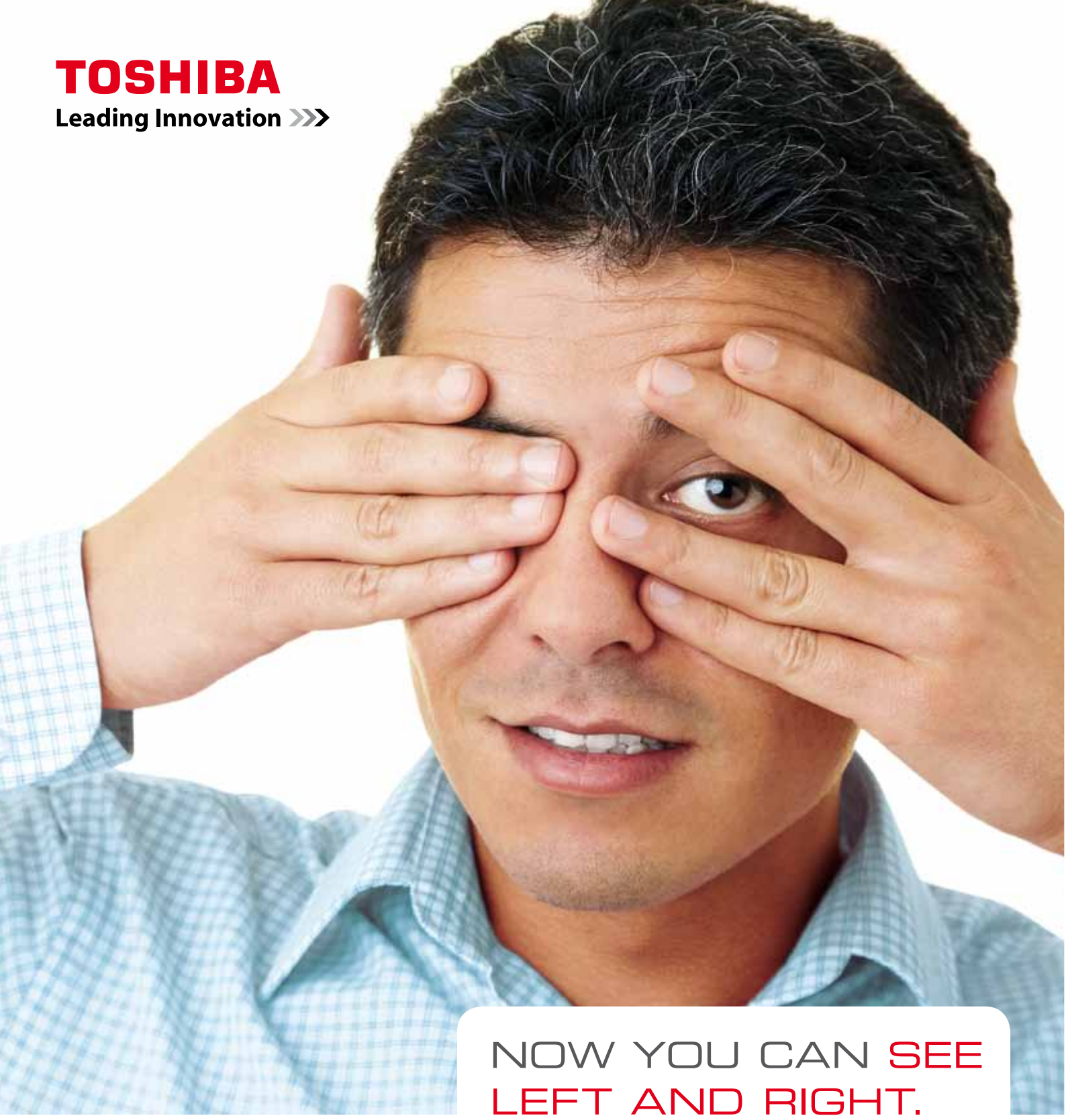

NOW YOU CAN SEE LEFT AND RIGHT.

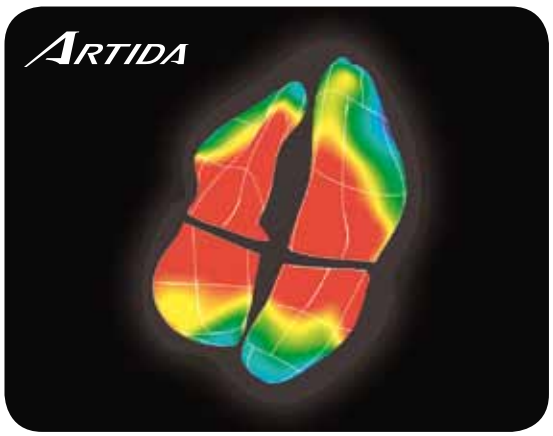

With 3D Wall Motion Tracking you can assess global and regional LV function in just a few easy steps – dynamically and in 3D. The method is clinically validated and numerous scientific publications prove its clinical relevance in assessing LV myocardial function. With the new version of Artida we have upgraded 3D Wall Motion Tracking to all chambers of the left and right heart. So looking at a heart now, your vision is 20/20.

Contact your local Toshiba representative for a demonstration and experience the future of 3D myocardial function assessment. www.toshiba-medical.eu

3DWMT

Made for Life

ULTRASOUND CT MRI X-RAY SERVICES